

# LPA<sub>4</sub>/p2y<sub>9</sub>/GPR23 Mediates Rho-dependent Morphological Changes in a Rat Neuronal Cell Line\*

Received for publication, June 21, 2006, and in revised form, December 15, 2006. Published, JBC Papers in Press, December 17, 2006, DOI 10.1074/jbc.M610767200

Keisuke Yanagida<sup>†</sup>, Satoshi Ishii<sup>†§1</sup>, Fumie Hamano<sup>†</sup>, Kyoko Noguchi<sup>‡</sup>, and Takao Shimizu<sup>‡</sup>

From the <sup>†</sup>Department of Biochemistry and Molecular Biology, Faculty of Medicine, the University of Tokyo and the <sup>‡</sup>Precursory Research for Embryonic Science and Technology (PRESTO) of Japan Science and Technology Agency, 7-3-1 Hongo, Bunkyo-ku, Tokyo 113-0033, Japan

Lysophosphatidic acid (LPA) is a potent lipid mediator that evokes a variety of biological responses in many cell types via its specific G protein-coupled receptors. In particular, LPA affects cell morphology, cell survival, and cell cycle progression in neuronal cells. Recently, we identified p2y<sub>9</sub>/GPR23 as a novel fourth LPA receptor, LPA<sub>4</sub> (Noguchi, K., Ishii, S., and Shimizu, T. (2003) *J. Biol. Chem.* 278, 25600–25606). To assess the functions of LPA<sub>4</sub> in neuronal cells, we used rat neuroblastoma B103 cells that lack endogenous responses to LPA. In B103 cells stably expressing LPA<sub>4</sub>, we observed G<sub>q/11</sub>-dependent calcium mobilization, but LPA did not affect adenylyl cyclase activity. In LPA<sub>4</sub> transfectants, LPA induced dramatic morphological changes, *i.e.* neurite retraction, cell aggregation, and cadherin-dependent cell adhesion, which involved Rho-mediated signaling pathways. Thus, our results demonstrated that LPA<sub>4</sub> as well as LPA<sub>1</sub> couple to G<sub>q/11</sub> and G<sub>12/13</sub>, whereas LPA<sub>4</sub> differs from LPA<sub>1</sub> in that it does not couple to G<sub>i/o</sub>. Through neurite retraction and cell aggregation, LPA<sub>4</sub> may play a role in neuronal development such as neurogenesis and neuronal migration.

Lysophosphatidic acid (LPA,<sup>2</sup> 1- or 2-acyl-*sn*-glycero-3-phosphate) is a naturally occurring bioactive lipid mediator that controls growth, motility, and differentiation (1). LPA plays important roles in many biological processes, such as brain development, oncogenesis, wound healing, and immune functions (2). The effects of LPA on target cells are mediated by activation of its specific G protein-coupled receptors (GPCRs). The LPA<sub>1</sub> (3), LPA<sub>2</sub> (4), and LPA<sub>3</sub> (5) receptors are the major members of the endothelial differentiation gene (EDG) family that interact with LPA. Pharmacological studies suggest that

both LPA<sub>1</sub> and LPA<sub>2</sub> couple to at least three types of G proteins, G<sub>i/o</sub>, G<sub>q</sub>, and G<sub>12/13</sub>, whereas LPA<sub>3</sub> couples to G<sub>i/o</sub> and G<sub>q</sub> but not G<sub>12/13</sub> (6). Depending on the functional coupling of a given LPA receptor to G proteins, LPA activates diverse signaling cascades involving phosphoinositide 3-kinase, phospholipase C, mitogen-activated protein kinase, Rho family GTPase, and adenylyl cyclase (2, 7).

LPA is present in the brain at relatively high levels compared with other organs (8, 9). LPA influences the cell morphology of several neuronal cell lines, neural progenitors, and primary neurons (10). It has also been reported that LPA affects electrophysiology, cell survival, and cell cycle progression in neuronal cells (10, 11). Targeted deletion of LPA<sub>1</sub> in mice produces olfactory deficits (12) and a behavioral abnormality (13). Furthermore, the use of LPA<sub>1</sub> knockouts revealed that LPA<sub>1</sub> is involved in the initiation of neuropathic pain (14). Exposure of the developing cerebral cortex to LPA produces dramatic changes in the folding of the brain, which do not occur in LPA<sub>1</sub> and LPA<sub>2</sub> double knockouts (15). However, the LPA receptor subtypes responsible for some neuronal effects have not been identified (16–18).

Recently, we identified p2y<sub>9</sub>/GPR23 as a fourth LPA receptor (LPA<sub>4</sub>) that is structurally distinct from the three LPA receptors of the EDG family (19). The expressed sequence tag cDNA encoding LPA<sub>4</sub> was originally isolated from human brain (20, 21), and LPA<sub>4</sub> expression has been detected in rat embryonic hippocampal neurons (22) and immortalized hippocampal progenitor cells (18). These facts suggest that LPA<sub>4</sub> may have important roles in neurodevelopmental processes such as neurogenesis and neuronal migration. However, only very limited information is available regarding its physiological and biological functions. To assess the functional roles of LPA<sub>4</sub> in neuronal cells, we generated B103 cells stably expressing LPA<sub>4</sub>. This study demonstrates that treatment of the LPA<sub>4</sub>-expressing cells with LPA leads to morphological changes, including cell rounding and cadherin-dependent cell adhesion following cell aggregation, both of which are mediated by the Rho/Rho-associated kinase (ROCK) pathway. The effects of LPA<sub>4</sub> on the morphology of the neuronal cells were clearly distinct from those of LPA<sub>1</sub>, probably because LPA<sub>4</sub> does not couple to G<sub>i/o</sub>.

## EXPERIMENTAL PROCEDURES

**Cell Culture**—B103 rat neuroblastoma cells were kindly provided by Dr. J. Chun (The Scripps Research Institute, La Jolla, CA). B103 cells expressing each of the LPA receptors were maintained on poly-L-lysine-coated 100-mm dishes (Iwaki,

\* This work was supported by grants-in-aid from the Ministry of Education, Culture, Sports, Science, and Technology of Japan (to T. S. and S. I.). The costs of publication of this article were defrayed in part by the payment of page charges. This article must therefore be hereby marked "advertisement" in accordance with 18 U.S.C. Section 1734 solely to indicate this fact.

<sup>1</sup> To whom correspondence should be addressed: Dept. of Biochemistry and Molecular Biology, Faculty of Medicine, The University of Tokyo, 7-3-1 Hongo, Bunkyo-ku, Tokyo 113-0033, Japan. Tel.: 81-3-5802-2925; Fax: 81-3-3813-8732; E-mail: mame@m.u-tokyo.ac.jp.

<sup>2</sup> The abbreviations used are: LPA, lysophosphatidic acid; GPCR, G protein-coupled receptor; EDG, endothelial differentiation gene; ROCK, Rho-associated kinase; DMEM, Dulbecco's modified Eagle's medium; PTX, pertussis toxin; HA, hemagglutinin; PBS, phosphate-buffered saline; BSA, bovine serum albumin; HBSS, Hank's balanced salt solution; IBMX, 2-isobutyl-1-methylxanthine; [Ca<sup>2+</sup>]<sub>i</sub>, intracellular Ca<sup>2+</sup> concentration; EGFP, enhanced green fluorescence protein; S1P, sphingosine 1-phosphate; MEMF, mouse embryonic meningeal fibroblast; MSF, mouse skin fibroblast.

Tokyo, Japan) in Dulbecco's modified Eagle's medium (DMEM) (Sigma) supplemented with 10% fetal bovine serum (BioWhittaker, Walkersville, MD) and 0.3 mg/ml G418 (Wako, Osaka, Japan). For some experiments, cells were pretreated with 100 ng/ml pertussis toxin (PTX) (List Biological Laboratories, Campbell, CA; from a 400  $\mu$ g/ml stock in 10 mM Tris-HCl (pH 7.4) and 2 M urea stored at 4 °C) for 12 h, 5  $\mu$ M YM-254890 (a novel  $G_{q/11}$  inhibitor (23), a kind gift from Dr. J. Takasaki, Astellas Pharma Inc., Tokyo, Japan; from a 10 mM stock in dimethyl sulfoxide (Sigma) stored at -30 °C) for 10 min, or 5  $\mu$ M Y-27632 (Calbiochem; from a 5 mM stock in water stored at -30 °C) for 10 min. Pretreatment with vehicles of PTX and YM-254890 was used as a control.

**Stable Expression of  $LPA_1$  and  $LPA_4$** —A DNA fragment containing the entire open reading frame of  $LPA_1$  (NCBI accession number NM\_001401) was first amplified from a cDNA prepared from human brain poly(A)<sup>+</sup> RNA (Clontech) by PCR using *Pfu* turbo DNA polymerase (Stratagene, La Jolla, CA) and oligonucleotides (sense primer, 5'-AAGAAATTTGTCTCC-CGTAGCTCT-3' and antisense primer, 5'-CATGAGTTGAC-TTTTCTCTCTCTC-3'). The entire open reading frame of  $LPA_1$  with an additional sequence encoding a hemagglutinin (HA) epitope (YPYDVPDYA) at the 5'-end was subsequently amplified from the resultant PCR products using KOD-Plus DNA polymerase (Toyobo, Osaka, Japan) and oligonucleotides (sense primer containing the KpnI and HA tag sequences, 5'-GGGGTACCGCCATGTACCCCTACGACG-TGCCGACTACGCCGCTGCCATCTCTACTTCC-3' and antisense primer containing the SpeI sequence, 5'-GGAC-TAGTCTAAACCACAGAGTGGTCATT-3'). The resultant DNA fragment was digested with KpnI and SpeI and subsequently cloned into the mammalian expression vector pCXN2.1, a slightly modified version of pCXN2 (24) with multiple cloning sites, between the KpnI and SpeI sites. HA-tagged human  $LPA_4$  cDNA was constructed and cloned into pCXN2.1 as described previously (19). B103 cells were transfected using the Lipofectamine 2000 reagent (Invitrogen). After 48 h, the transient expression of the HA epitope on the cell surface was confirmed by flow cytometric analysis (EPICS XL, Beckman Coulter, Fullerton, CA) with the 3F10 rat monoclonal anti-HA antibody (Roche Applied Science) and phycoerythrin-labeled anti-rat IgG (Beckman Coulter) as the secondary antibody. Stable transfectants were selected with 1 mg/ml G418 for 26 days. After staining the drug-resistant cells as described above, a group of HA-positive cells was sorted by flow cytometry (EPICS ALTRA, Beckman Coulter) and maintained with 0.3 mg/ml G418. Three weeks later, a second round of sorting was performed; the twice-immunopurified cells were used for experiments (termed B103- $LPA_1$  and B103- $LPA_4$  cells).

**Binding Assay**—Binding assay was done essentially as described previously (19), with minor modifications. Cells ( $4 \times 10^6$ ) were seeded in collagen-coated 100-mm plates (Iwaki), followed by 24 h of serum starvation. The cells were washed with phosphate-buffered saline (PBS) twice and scraped off. After further washing with binding buffer (25 mM HEPES-NaOH (pH 7.4), 10 mM  $MgCl_2$ , and 0.25 M sucrose), the cells were suspended in the buffer with additional protease inhibitor mixture (Complete, Roche Applied Science), sonicated three

## $LPA_4$ Changes the Morphology of Neuronal Cells

times at 15 watts for 30 s, and centrifuged at  $800 \times g$  for 10 min at 4 °C. The supernatant was further centrifuged at  $10^5 \times g$  for 60 min at 4 °C, and resultant pellet was homogenized in ice-cold binding buffer. Binding assays were performed in 96-well plates in triplicate. 20  $\mu$ g each of the membrane fractions from the twice-immunopurified cells was incubated in binding buffer containing 0.25% bovine serum albumin (BSA) (fatty acid-free, very low endotoxin grade; Serologicals Proteins, Kankakee, IL) with 2-fold serial dilutions (50–3.125 nM) of [<sup>3</sup>H]LPA (1-oleoyl[oleoyl-9,10-<sup>3</sup>H]LPA, 57 Ci/mmol; PerkinElmer Life Sciences) for 60 min at 4 °C. The bound [<sup>3</sup>H]LPA was collected onto a Unifilter-96-GF/C (PerkinElmer Life Sciences) using a MicroMate 196 harvester (Packard Instrument Co.). The filter was then rinsed 10 times with ice-cold binding buffer and dried for 12 h at 50 °C. 25  $\mu$ l of MicroScint-0 scintillation mixture (PerkinElmer Life Sciences) was added per well. The radioactivity that remained on the filter was measured with TopCount microplate scintillation counter (Packard Instrument Co.). Total and nonspecific bindings were evaluated in the absence and presence of 10  $\mu$ M unlabeled LPA [1-oleoyl (18:1)-LPA; Cayman Chemical, Ann Arbor, MI], respectively. The specific binding value (disintegrations/min) was calculated by subtracting the nonspecific binding value (disintegrations/min) from the total binding value (disintegrations/min). A dissociation constant ( $K_d$ ) and a maximum binding capacity ( $B_{max}$ ) were calculated by Scatchard analysis.  $B_{max}$  and  $K_d$  values for B103- $LPA_1$  cells were 0.8 pmol/mg protein and 18 nM, respectively. Those for B103- $LPA_4$  cells were 6.0 pmol/mg protein and 58 nM. No specific binding was observed in vector-transfected B103 cells (B103-vector cells).

**cAMP Measurement**—Cells ( $3.2 \times 10^4$ ) were seeded in collagen-coated 96-well plates (Iwaki), followed by 24 h of serum starvation. To determine whether LPA receptors mediate the inhibition of adenylyl cyclase, an AlphaScreen cAMP assay kit (PerkinElmer Life Sciences) was used as recommended in the manufacturer's instructions. The cells were washed twice with buffer A (Hanks' balanced salt solution (HBSS) containing 25 mM HEPES-NaOH (pH 7.4) and 0.1% BSA (Serologicals Proteins)) and incubated in 100  $\mu$ l of buffer A containing 0.5 mM 3-isobutyl-1-methylxanthine (IBMX) (from a 20 mM stock in dimethyl sulfoxide stored at -30 °C) (Sigma) for 15 min at room temperature. The reaction was initiated by adding 50  $\mu$ l of various concentrations of LPA in buffer A with 50  $\mu$ M forskolin (Wako; from a 10 mM stock in dimethyl sulfoxide stored at -30 °C). After 30 min of incubation at room temperature, the reaction was terminated by adding 16.6  $\mu$ l of 10% Tween 20, followed by overnight storage at 4 °C. After centrifugation at  $800 \times g$  for 5 min, the cAMP concentration in the supernatant was measured in quadruplicate with a fusion system (PerkinElmer Life Sciences). To determine whether LPA receptors mediate the stimulation of adenylyl cyclase, the cAMP Biotrak EIA system (Amersham Biosciences) was used as recommended in the manufacturer's instructions. The cells were washed twice with HEPES-Tyrode's buffer (25 mM HEPES-NaOH (pH 7.4), 140 mM NaCl, 2.7 mM KCl, 1 mM  $CaCl_2$ , 0.49 mM  $MgCl_2$ , 12 mM  $NaHCO_3$ , 0.37 mM  $NaH_2PO_4$ , and 5.6 mM D-glucose) containing 0.1% BSA (HEPES-Tyrode's BSA buffer) and incubated in 100  $\mu$ l of HEPES-Tyrode's BSA buffer con-

## LPA<sub>4</sub> Changes the Morphology of Neuronal Cells

taining 0.5 mM IBMX for 15 min at 37 °C. The reaction was initiated by adding 100  $\mu$ l of various concentrations of LPA in HEPES-Tyrod's BSA buffer. After 30 min of incubation at 37 °C, the reaction was terminated by adding 25  $\mu$ l of lysis buffer. Cell lysates in a volume of 100  $\mu$ l were used to determine the cAMP concentration using an enzyme immunoassay method.

**Ca<sup>2+</sup> Measurement**—Cells serum-starved for 24 h were detached with PBS containing 2 mM EDTA, washed with HEPES-Tyrod's buffer, and then loaded with 3  $\mu$ M Fura-2 AM (Dojindo, Kumamoto, Japan) in HEPES-Tyrod's BSA buffer for 1 h at 37 °C. The cells were washed twice and resuspended in HEPES-Tyrod's BSA buffer at a density of  $1 \times 10^6$  cells/ml. The cell suspension (0.5 ml) was applied to a CAF-100 spectrofluorometer (Jasco, Tokyo, Japan), and 5  $\mu$ l of 100  $\mu$ M LPA in HEPES-Tyrod's BSA buffer was added. The intracellular Ca<sup>2+</sup> concentration ([Ca<sup>2+</sup>]<sub>i</sub>) was measured as the ratio of emission fluorescence at 500 nm in response to excitation at 340 and 380 nm.

**Cell Rounding Assay**—Cells ( $1 \times 10^4$ ) were seeded in poly-D-lysine-coated 12-well plates (BD Biosciences). After 24 h of incubation, the cells were washed three times with DMEM containing 0.1% BSA and serum-starved for 24 h. Three hours after a medium change, the cells were treated with 1  $\mu$ M LPA for 15 min. The cells were examined for a round cell morphology lacking any neurite extensions or filopodia. Extended neurites were defined as having a length greater than the cell body. The number of rounded cells was expressed as a percentage of the observed cells (>200 cells/well).

**Rho Inhibition Study**—Cells ( $5 \times 10^5$ ) were seeded in poly-L-lysine-coated 35-mm dishes (Iwaki) in DMEM supplemented with 10% fetal bovine serum. After 24 h, either the *Clostridium botulinum* C3 exoenzyme expression vector (pEF-C3) (25) (a kind gift from Dr. S. Narumiya, Kyoto University, Kyoto, Japan) or the corresponding control vector (pEF-BOS) (26) (a kind gift from Dr. S. Nagata, Osaka University, Osaka, Japan) was cotransfected with an enhanced green fluorescent protein (EGFP) expression vector (pEGFP-C1; Clontech) at a 4:1 weight ratio, with 3  $\mu$ g of total DNA, using the Lipofectamine 2000 reagent (Invitrogen). After 24 h, the cells were seeded in poly-D-lysine-coated 12-well plates and cultured for 24 h. The cells were then serum-starved for 12 h and treated with 1  $\mu$ M LPA for 15 min. Following fixation with 1% paraformaldehyde for 15 min at 4 °C, EGFP images were obtained using a fluorescence microscope (Diaphoto, Nikon, Tokyo, Japan). EGFP-positive cells were examined for a round morphology without any neurite extensions or filopodia. At least 20 different fields were observed with a minimum of 100 EGFP-positive cells. The number of rounded cells was expressed as a percentage of the EGFP-positive cells.

**Quantification of Cell Clustering**—The degree of cell clustering was quantified by observing the distribution of the cell nuclei. Cells ( $1.5 \times 10^5$ ) were seeded in poly-D-lysine-coated 24-well plates (BD Biosciences). After 24 h of incubation, the cells were washed three times with DMEM containing 0.1% BSA and serum-starved for 24 h. Three hours after a medium change, the cells were treated with 1  $\mu$ M LPA for 3 h, followed by fixation and staining with a Diff-Quik kit (Kokusai Shiyaku,

Kobe, Japan). The distribution of the cells was mapped in rectangular areas (1710  $\times$  1290  $\mu$ m) by photographing the cultures (Cool Pix 990, Nikon). Each map was overlaid with grids at equal intervals (30  $\mu$ m) and divided into 2451 unit squares. The randomness in spatial distribution was tested by counting the number of unit squares containing at least one nucleus. The intensity of the cell clustering was expressed as the percentage of the unit squares without any nuclei.

**Cell Dissociation Assay**—The Ca<sup>2+</sup> sensitivity of cell-cell adhesion was estimated using trypsin treatment in the presence of either CaCl<sub>2</sub> (TC treatment) or EDTA (TE treatment) as described (27, 28), with minor modifications. Briefly,  $5 \times 10^5$  cells were seeded in poly-D-lysine-coated 35-mm dishes (BD Biosciences) and cultured overnight. After 24 h of serum starvation, the cells were stimulated with 1  $\mu$ M LPA for 2 h and washed with HBSS containing either 2 mM CaCl<sub>2</sub> or 2 mM EDTA. The washed cells were treated with 0.01% trypsin for 30 min at 37 °C and then dissociated by pipetting 10 times gently in 1 ml of HBSS with 0.01% trypsin. The number of cell clusters was counted with a particle counter (Beckman Coulter). The degree of cell-cell adhesion was expressed as the ratio of particles in the TC condition to particles in the TE condition (TC/TE). Negative control experiments without LPA treatment were also performed.

**Western Blotting**—Cells ( $4 \times 10^6$ ) were seeded in poly-L-lysine-coated 100-mm dishes. Following 24 h of serum starvation, the cells were treated with 1  $\mu$ M LPA for 3 h, washed twice with PBS, and harvested in buffer B (25 mM HEPES-NaOH (pH 7.4), 10 mM MgCl<sub>2</sub>, and 0.25 M sucrose). The cells were centrifuged at 800  $\times$  g for 10 min at 4 °C, suspended in ice-cold buffer B containing 20  $\mu$ M 4-aminodiphenylmethylsulfonyl fluoride (Sigma) and a protease inhibitor mixture (Complete, Roche Applied Science), and sonicated three times for 30 s each at 4 °C. The cell debris was removed by centrifugation at 800  $\times$  g for 10 min at 4 °C. The protein concentration of the homogenate was determined with a Bradford assay (Bio-Rad) using BSA as a standard. Five micrograms of protein sample containing 5% 2-mercaptoethanol was analyzed by 7.5% SDS-PAGE followed by transfer to a polyvinylidene difluoride membrane (Millipore Corp., Bedford, MA). The membrane was blocked with 5% skim milk (Difco) and probed with a mouse monoclonal antibody against N-cadherin or E-cadherin (BD Biosciences). The bands were visualized with an ECL chemiluminescence detection system (Amersham Biosciences) using horseradish peroxidase-conjugated anti-mouse IgG (Amersham Biosciences).

**Immunofluorescence**—Cells ( $3 \times 10^5$ ) were seeded into poly-L-lysine-coated glass-bottomed 35-mm dishes (Matsunami, Tokyo, Japan) and serum-starved for 24 h. Following stimulation with 1  $\mu$ M LPA for 3 h at 37 °C, the cells were fixed with 4% paraformaldehyde for 20 min at 4 °C and rinsed twice with ice-cold PBS. Subsequently, the cells were incubated with a mouse monoclonal antibody against N-cadherin in PBS containing 1/4 $\times$  permeabilization reagent (Beckman Coulter) for 1 h at room temperature. The primary antibody staining was visualized with an Alexa 488-conjugated goat anti-mouse IgG (Invitrogen). Images were obtained using an LSM510 laser-scanning confocal microscope (Carl Zeiss, Jena, Germany) equipped with an argon laser as the light source.

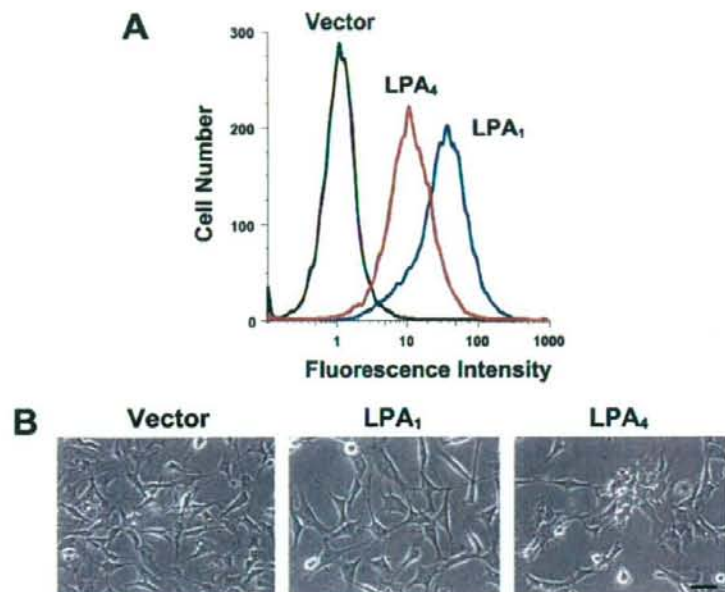


**FIGURE 1. Stable expression of LPA<sub>1</sub> or LPA<sub>4</sub> in B103 cells results in distinct morphologies.** A, flow cytometry analysis. B103 cells were stably transfected with the expression vectors for LPA<sub>1</sub> or LPA<sub>4</sub>, each tagged with an HA epitope at the N terminus. After staining with an anti-HA antibody and a phycoerythrin-conjugated secondary antibody, HA-positive cells were sorted with a cell sorter and then subcultured. Data shown are the surface expression levels of the HA epitope in subcultured polyclonal cells obtained by the second round of cell sorting. Empty vector-transfected polyclonal cells served as a negative control. B, morphology of B103-vector, B103-LPA<sub>1</sub>, and B103-LPA<sub>4</sub> cells in serum-containing medium. The cells were photographed 24 h after seeding. Each stable cell line showed similar growth rate. Bar, 40  $\mu$ m.

**Statistical Analysis**—All values in the figures are expressed as means  $\pm$  S.E. To determine statistical significance, the values were compared by analysis of variance followed by Tukey-Kramer test using Prism 4 software (GraphPad Software, San Diego, CA). The differences were considered significant if *p* values were less than 0.05.

## RESULTS

**Stable Expression of LPA<sub>1</sub> and LPA<sub>4</sub> in B103 Cells Results in Different Morphologies in Serum-containing Medium**—To address the functional roles of LPA<sub>4</sub> in neuronal cells, B103 rat neuroblastoma cells were stably transfected with the expression vector for either LPA<sub>1</sub> or LPA<sub>4</sub>. B103 cells were selected because they lack endogenous responses to LPA (29, 30). Consistently, no specific binding was observed in B103-vector cells in the radioligand binding assays (see "Experimental Procedures"). To determine the intrinsic gene expression profiles of LPA receptors in B103 cells, we performed a reverse transcription-PCR analysis of total cellular RNA from the cells. Although LPA<sub>4</sub> mRNA expression was slightly detected, no mRNA expression of the other three receptors, LPA<sub>1</sub>, LPA<sub>2</sub>, and LPA<sub>3</sub>, was observed (data not shown). This finding is consistent with a recent report by Tsukahara *et al.* (31). The apparent discrepancy between the expression of LPA<sub>4</sub> and the lack of response to LPA might occur because the expression of LPA<sub>4</sub> is too low to respond to LPA. Alternatively, post-transcriptional/translational modifications (32) may produce discordance between

mRNA and protein expression. Thus, we discounted the low expression of LPA<sub>4</sub> in B103 cells and took advantage of their unresponsiveness to LPA and their neuronal nature for the purpose of examining the functional roles of LPA<sub>4</sub> in neuronal cells.

For the construction of stably transfected cell lines, LPA<sub>1</sub> and LPA<sub>4</sub> were tagged with an HA epitope at the N terminus to enable us to determine the levels of expression on the cell surfaces. Fluorescence-activated cell sorting enriched a polyclonal population of the drug-resistant cells that expressed each LPA receptor. These populations of stable clones are free of any clonal deviation that could cause functional variations. Following two rounds of cell sorting, we observed that the fluorescence intensity of B103-LPA<sub>4</sub> cells was higher than that of B103-LPA<sub>1</sub> cells (Fig. 1A), although the  $B_{max}$  value for B103-LPA<sub>1</sub> cells (0.8 pmol/mg of protein) was lower than that for B103-LPA<sub>4</sub> cells (6.0 pmol/mg of protein). The apparent discrepancy might be because of

two possibilities as follows: the usage of organellar membrane-rich microsomal fractions and the difference in HA antibody immunoreactivity to the HA epitope tagged to two receptors. To confirm that no expression of the other subtypes of LPA receptors was enhanced secondary to the transfection, reverse transcription-PCR was performed with specific primers for LPA<sub>1</sub>, LPA<sub>2</sub>, LPA<sub>3</sub>, and LPA<sub>4</sub> in B103-vector, B103-LPA<sub>1</sub>, and B103-LPA<sub>4</sub> cells. As in the parental B103 cells, we observed only a low expression of LPA<sub>4</sub> and virtually no expression of the other LPA receptors in all of the transfected cell lines (data not shown).

Although these stably transfected cell lines showed similar growth rates (data not shown), they showed distinctly different morphologies in serum-containing medium (Fig. 1B). As reported previously (33), B103-LPA<sub>1</sub> cells displayed a flattened and more migratory morphology compared with B103-vector cells. Interestingly, B103-LPA<sub>4</sub> cells had an epithelial like morphology and appeared to adhere more tightly to each other than B103-vector cells. These observations suggest that LPA<sub>1</sub> and LPA<sub>4</sub> have distinct signaling pathways that produce different cell morphologies.

**LPA<sub>4</sub> Does Not Affect Adenylyl Cyclase Activity in B103 Cells**—We examined whether LPA<sub>4</sub> mediates the inhibition of adenylyl cyclase activity in B103 cells, as the other three LPA receptors do (30) (Fig. 2A). In B103-LPA<sub>1</sub> cells, LPA caused a dose-dependent inhibition of adenylyl cyclase activity with IC<sub>50</sub> values below 10 nM (Fig. 2A). This inhibition was completely

## LPA<sub>4</sub> Changes the Morphology of Neuronal Cells

blocked by PTX treatment, indicating the primary role of G<sub>i/o</sub> proteins. However, LPA at concentrations up to 10 μM did not blunt the forskolin-driven rises in cAMP accumulation in either B103-vector or B103-LPA<sub>4</sub> cells, suggesting that LPA<sub>4</sub> does not couple to G<sub>i/o</sub> proteins.

Previously, we reported that LPA induces cAMP accumulation in LPA<sub>4</sub>-expressing Chinese hamster ovary cells (19). However, LPA did not elevate basal cAMP levels in either B103-LPA<sub>4</sub> cells or B103-LPA<sub>1</sub> cells (Fig. 2B), suggesting that neither LPA<sub>1</sub> nor LPA<sub>4</sub> couples to G<sub>s</sub> in B103 cells.

**LPA<sub>1</sub> and LPA<sub>4</sub> Mediate Ca<sup>2+</sup> Mobilization via Distinct Signaling Pathways**—LPA has been shown to induce intracellular Ca<sup>2+</sup> mobilization in many cell types (34), and all EDG family

LPA receptor subtypes mediate Ca<sup>2+</sup> mobilization when expressed in B103 cells (30). We therefore examined whether LPA<sub>4</sub> mediates Ca<sup>2+</sup> mobilization in B103 cells. Although B103-vector cells displayed no response to 1 μM LPA, increases in [Ca<sup>2+</sup>]<sub>i</sub> were observed both in B103-LPA<sub>1</sub> and B103-LPA<sub>4</sub> cells (Fig. 3). LPA induces phospholipase C-mediated Ca<sup>2+</sup> mobilization via the PTX-sensitive G<sub>i/o</sub> and/or PTX-insensitive G<sub>q/11</sub>-mediated pathways (34). To examine the signaling pathways leading to Ca<sup>2+</sup> mobilization in B103-LPA<sub>1</sub> and B103-LPA<sub>4</sub> cells, we treated the cells with a G<sub>q/11</sub>-selective inhibitor, YM-254890 (23) (Fig. 3). ATP was used as a positive control, because ATP evokes Ca<sup>2+</sup> mobilization via P2Y receptors predominantly through G<sub>q/11</sub> (35). The LPA-induced Ca<sup>2+</sup> response in B103-LPA<sub>4</sub> cells and the ATP-induced Ca<sup>2+</sup> response in both transfected cell lines were completely abolished by pretreatment with 5 μM YM-254890 (Fig. 3). In B103-LPA<sub>1</sub> cells, YM-254890 only partially inhibited the LPA-induced response (Fig. 3), but the combination of PTX and YM-254890 produced complete inhibition (data not shown). The degree of inhibition with YM-254890 in B103-LPA<sub>1</sub> cells was not altered at higher concentrations (up to 20 μM; data not shown), indicating that 5 μM YM-254890 was sufficient to inhibit the activation of G<sub>q/11</sub> proteins. These results suggest that both G<sub>i/o</sub> and G<sub>q/11</sub> proteins mediate Ca<sup>2+</sup> mobilization in B103-LPA<sub>1</sub> cells, whereas G<sub>q/11</sub> is the dominant mediator of the response in B103-LPA<sub>4</sub> cells.

**Both LPA<sub>1</sub> and LPA<sub>4</sub> Mediate Cell Rounding via Rho-dependent and G<sub>i/o</sub>- and G<sub>q/11</sub>-independent Pathways**—LPA induces rapid growth cone collapse, neurite retraction, and neuronal cell rounding in several neuronal cell types

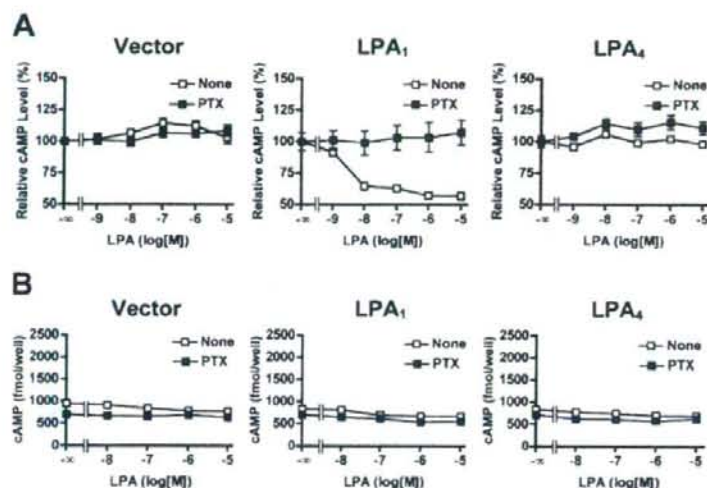


**FIGURE 2. LPA does not affect adenyl cyclase activity in B103-LPA<sub>4</sub> cells.** *A*, failure of LPA to inhibit forskolin-induced cAMP accumulation in B103-LPA<sub>4</sub> cells. Serum-starved B103-vector, B103-LPA<sub>1</sub>, and B103-LPA<sub>4</sub> cells were stimulated with increasing concentrations of LPA in the presence of 0.5 mM IBMX and 50 μM forskolin. After a 30-min incubation at room temperature, the cells were solubilized, and cAMP concentrations in the cell lysates were measured. Forskolin-induced cAMP accumulation in the absence of LPA was set to 100%. Where indicated, the cells were pretreated with 100 ng/ml PTX for 24 h. Data are means ± S.E. (*n* = 4) of a representative of three independent experiments with similar results. *B*, failure of LPA to induce cAMP accumulation in B103-LPA<sub>4</sub> cells. Serum-starved B103-vector, B103-LPA<sub>1</sub>, and B103-LPA<sub>4</sub> cells were stimulated with increasing concentrations of LPA in the presence of 0.5 mM IBMX. After a 30-min incubation at room temperature, the cells were solubilized, and cAMP concentrations in the cell lysates were measured. The cells were pretreated with 100 ng/ml PTX for 24 h. Data are representative of three independent experiments with similar results.

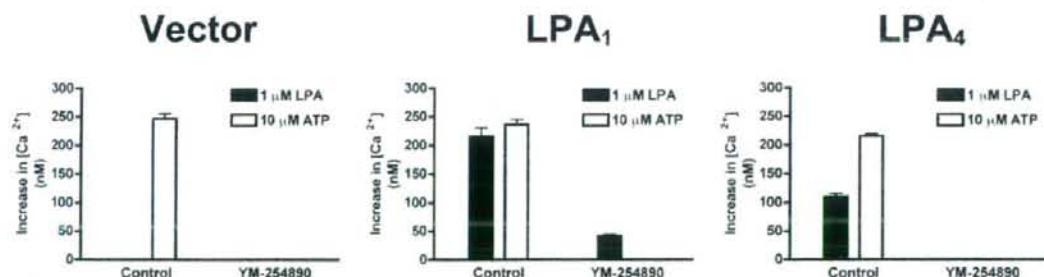


**FIGURE 3. LPA<sub>4</sub>-mediated Ca<sup>2+</sup> mobilization is entirely dependent on G<sub>q/11</sub> proteins.** B103-vector, B103-LPA<sub>1</sub>, and B103-LPA<sub>4</sub> cells were serum-starved, loaded with 3 μM Fura-2-AM, and stimulated with 1 μM LPA or 10 μM ATP. Where indicated, the cells were pretreated with 5 μM YM-254890 for 10 min. Data are means ± S.E. (*n* = 3) of a representative of three independent experiments with similar results.

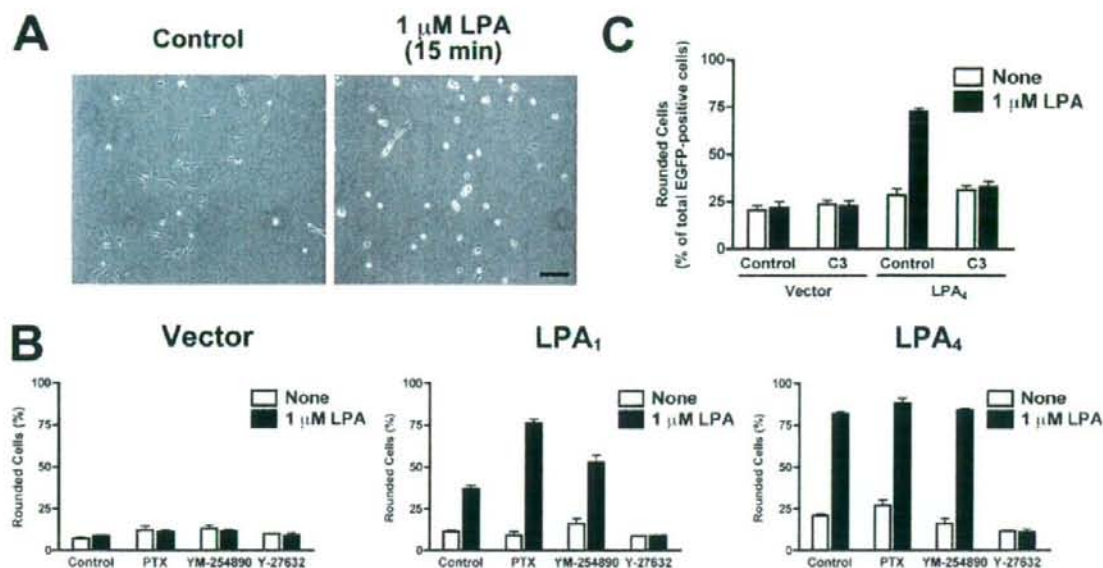


**FIGURE 4. LPA induces cell rounding in B103-LPA<sub>4</sub> cells through a G<sub>12/13</sub>-Rho-ROCK-dependent pathway.** *A*, induction of cell rounding in B103-LPA<sub>4</sub> cells. Serum-starved B103-LPA<sub>4</sub> cells were stimulated with 1 μM LPA for 15 min. *Bar*, 100 μm. *B*, effects of PTX, YM-254890, and Y-27632 on LPA-induced cell rounding in B103-vector, B103-LPA<sub>1</sub>, and B103-LPA<sub>4</sub> cells. The cells were pretreated with either 100 ng/ml PTX for 24 h, 5 μM YM-254890 for 10 min, or 5 μM Y-27632 for 10 min. The percentages of rounded cells among >200 cells are shown. Data are means ± S.E. (*n* = 3) of a representative of three independent experiments with similar results. *C*, effects of C3 exoenzyme on LPA-induced cell rounding in B103-LPA<sub>4</sub> cells. Either the C3 exoenzyme expression vector or the corresponding control vector was cotransfected with the EGFP expression vector. The cells were seeded, serum-starved, and treated with 1 μM LPA for 15 min. Following the fixation, EGFP images were obtained using a fluorescence microscope. The percentages of rounded cells among >100 EGFP-positive cells are shown. Data are means ± S.E. (*n* = 3) of a representative of two independent experiments with similar results.

(10). Mouse LPA<sub>1</sub> and LPA<sub>2</sub> and human LPA<sub>1</sub> have been reported to mediate LPA-induced cell rounding in B103 cells (29, 30, 33); we examined whether human LPA<sub>4</sub> also mediates cell rounding in B103 cells by seeding cells at a low cell density (Fig. 4, *A* and *B*). Overexpression of LPA<sub>1</sub> and LPA<sub>4</sub> slightly increased the percentages of rounded cells even before LPA application. Within 15 min of LPA stimulation, about 80% of B103-LPA<sub>4</sub> cells became rounded and underwent neurite retraction (Fig. 4*A*). Cell rounding was observed in B103-LPA<sub>1</sub> cells as reported previously (33), but to a lesser degree than in B103-LPA<sub>4</sub> cells. LPA-induced cell rounding was not observed in B103-vector cells.

The role of Rho in LPA-induced cell rounding is now well established (36), and the G<sub>12/13</sub> types of heterotrimeric G proteins are known to be upstream activators of Rho proteins (1, 2, 7). On the other hand, there are reports that G<sub>q/11</sub> activation induces cell rounding through Rho-dependent (37) and -independent (38) pathways. To determine which G proteins and signaling molecules are involved in LPA-induced cell rounding, we pretreated the cells with PTX, YM-254890, and a ROCK inhibitor, Y-27632 (Fig. 4*B*). In B103-LPA<sub>4</sub> cells, neither PTX nor YM-254890 inhibited LPA-induced cell rounding; in contrast, Y-27632 completely inhibited this morphological change. Y-27632 also hampered LPA-induced cell rounding in B103-LPA<sub>1</sub> cells, whereas YM-254890 did not affect the number of rounded cells. Interestingly, pretreatment with PTX increased the degree of LPA-induced cell rounding in B103-LPA<sub>1</sub> cells. To confirm the involvement of Rho, B103-LPA<sub>4</sub> cells were

transfected with C3 exoenzyme, which inactivates Rho by ADP-ribosylation. The transfected cells were identified by cotransfection of an EGFP expression construct. C3 exoenzyme transfection blunted LPA-induced cell rounding in B103-LPA<sub>4</sub> cells, again indicating the involvement of Rho (Fig. 4*C*).

**LPA<sub>4</sub> Mediates ROCK-dependent Cell Aggregation**—As described earlier, B103-LPA<sub>4</sub> cells appeared to form aggregates in serum-containing medium to a greater extent than B103-vector cells (Fig. 1*B*). To determine whether the binding of LPA to LPA<sub>4</sub> mediates the induction of cell-cell adhesion, B103-LPA<sub>4</sub> cells at a medium cell density were stimulated with 1 μM LPA after 24 h of serum starvation. Although the rapid cell rounding after LPA application was difficult to evaluate at this cell density because of the formation of cell-cell contacts, LPA caused a slow but dramatic aggregation in B103-LPA<sub>4</sub> cells (Fig. 5*A*, *panel f*). The morphological change observed in B103-LPA<sub>4</sub> cells was transient, reaching a maximum 2–3 h after the treatment and then returning to the base line 24 h after the treatment (data not shown).

To investigate the signaling pathways downstream of LPA<sub>4</sub> that are involved in the cell aggregation, we treated B103-LPA<sub>4</sub> cells with several inhibitors. The LPA-induced morphological changes in B103-LPA<sub>4</sub> cells were completely prevented by Y-27632 (Fig. 5*A*, *panel o*). In contrast, neither PTX nor YM-254890 inhibited the cell aggregation (Fig. 5*A*, *panels i* and *j*). We quantified the degree of cell aggregation by examining the randomness in the spatial distribution of the cells (see the "Experimental Procedures"; Fig. 5*B*). These results suggest that

LPA<sub>4</sub> Changes the Morphology of Neuronal Cells

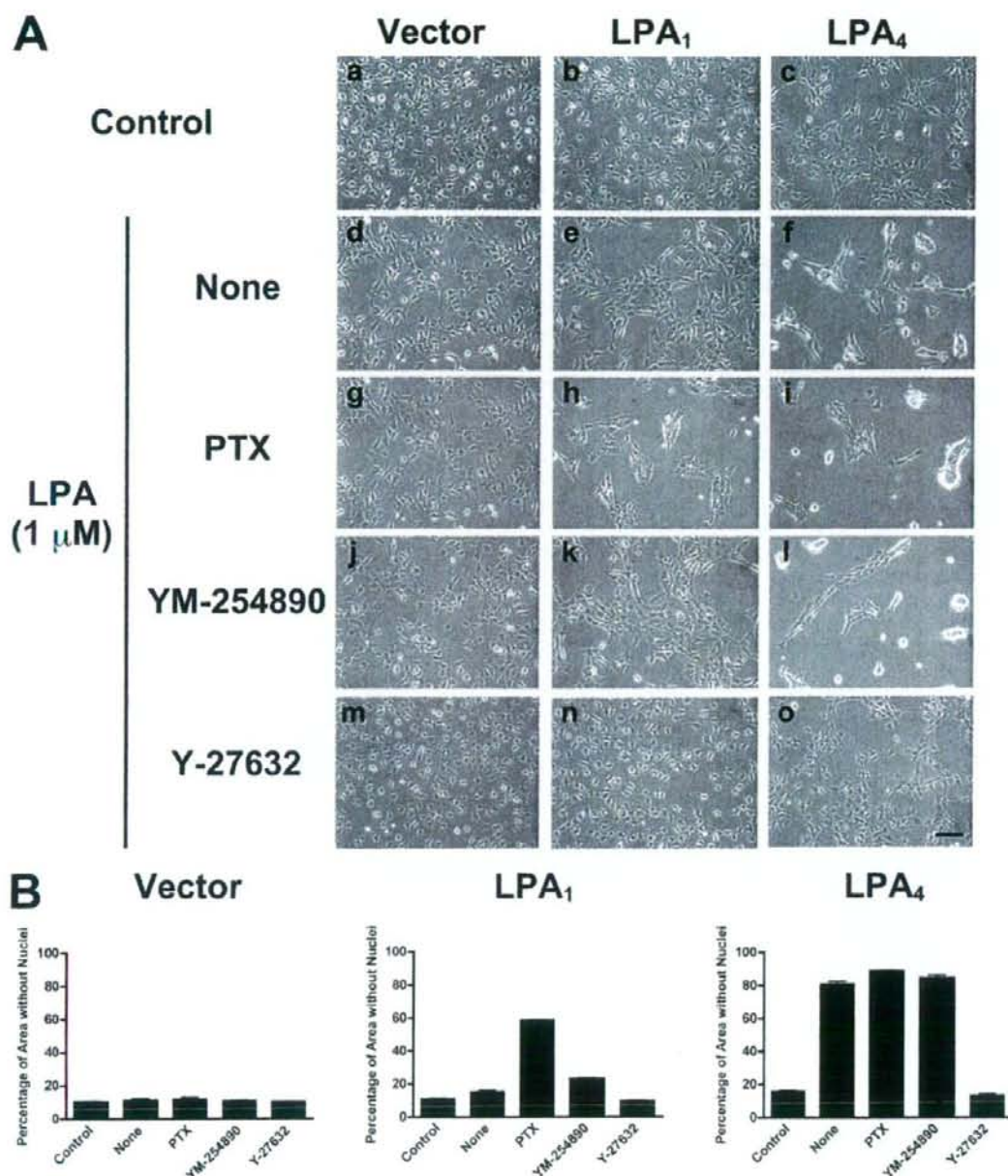


FIGURE 5. Cell aggregation in B103-LPA<sub>4</sub> cells is mediated by ROCK. *A*, cells were pretreated with either 100 ng/ml PTX for 24 h, 5  $\mu$ M YM-254890 for 10 min, or 5  $\mu$ M Y-27632 for 10 min prior to the LPA stimulation for 3 h. *Bar*, 100  $\mu$ m. *B*, quantification of cell clustering. Serum-starved cells were treated with 1  $\mu$ M LPA for 3 h, followed by fixation and staining. The intensity of the cell clustering was calculated as described under the "Experimental Procedures." Data are means  $\pm$  S.E. of three different rectangular areas (one rectangular area/well) of two independent experiments with similar results.

Rho mediates LPA-induced cell aggregation in B103-LPA<sub>4</sub> cells in a G<sub>i/o</sub>- and G<sub>q/11</sub>-independent manner. Rho regulates the reorganization of the actin cytoskeleton, which can modify the intensity of adhesion (28, 39). To examine whether the reorganization of the actin cytoskeleton was involved in this effect,

B103-LPA<sub>4</sub> cells were pretreated with cytochalasin D (an inhibitor of actin polymerization). In these cells, morphological changes were not observed after LPA stimulation, indicating that actin reorganization is involved in the LPA-induced cell aggregation (data not shown). Like B103-LPA<sub>4</sub> cells, PTX-

treated B103-LPA<sub>1</sub> cells became aggregated after LPA stimulation (Fig. 5A, panel h).

**LPA<sub>4</sub> Mediates N-cadherin-dependent Cell-Cell Adherence**—Through LPA-induced cell aggregation, B103-LPA<sub>4</sub> cells formed tightly compact aggregates (Fig. 5A, panel f), which dissociated very little after pipetting (data not shown). Cell-cell adhesion mechanisms can be Ca<sup>2+</sup>-dependent and Ca<sup>2+</sup>-independent, and cadherins are the major components of the Ca<sup>2+</sup>-dependent system. Cadherin-dependent adhesion was originally defined as being trypsin-resistant in the presence of Ca<sup>2+</sup> and trypsin-sensitive in the absence of Ca<sup>2+</sup> (40). We examined whether LPA-induced cell adhesion was mediated by cadherins using a cell dissociation assay, one of the adhesion assays for the evaluation of the cadherin activity (27, 28). We defined the TC/TE index as a ratio of the cell particle number after trypsin treatment in the presence of Ca<sup>2+</sup> (TC) to the number after trypsin treatment with EDTA (TE). Cadherin-dependent adhesion remains after trypsin-Ca<sup>2+</sup> treatment, whereas trypsin-EDTA treatment disrupts cell adhesion nearly completely. In either treatment, an increase in particles would occur when a large aggregate breaks into small particles by pipetting; the higher the number of particles, the lower the aggregation (adhesion). Thus, the TC/TE index is negatively correlated with cadherin-mediated adhesion. The aggregation level of B103-LPA<sub>4</sub> cells increased after LPA stimulation (Fig. 6A; note that the index inversely reflects cadherin activity). LPA treatment did not significantly affect the TC/TE index in either B103-vector cells or B103-LPA<sub>1</sub> cells. These results suggest that LPA increased the cadherin-mediated adhesive activity in B103-LPA<sub>4</sub> cells. Even LPA-untreated B103-LPA<sub>4</sub> cells had significantly more cadherin-dependent adhesion activity, *i.e.* a lower TC/TE index, than LPA-untreated B103-vector and B103-LPA<sub>1</sub> cells (Fig. 6A).

The cadherins constitute a large superfamily of molecules that includes the classic cadherins, the desmosomal cadherins, the protocadherins, and the cadherin-like signaling receptors (41). The levels of the two classic cadherins most commonly expressed in the nervous system, N- and E-cadherin, were determined by Western blotting of LPA-treated or -untreated B103 cells. Consistent with a previous report (42), these cells abundantly expressed N-cadherin (Fig. 6B), whereas E-cadherin was undetectable (data not shown). The expression level of N-cadherin was not up-regulated by LPA treatment in any of the transfected cell lines (Fig. 6B), and N-cadherin was intact in the cells undergoing TC treatment. In contrast, TE treatment resulted in complete digestion of N-cadherin (data not shown), as reported previously (43). We next examined whether LPA increases N-cadherin-mediated cell-cell contacts. LPA promoted the assembly of N-cadherin in the form of a thick, bright band at the cell-cell contact area in B103-LPA<sub>4</sub> cells but not in B103-vector cells (Fig. 6C).

## DISCUSSION

A number of studies have shown that LPA mediates morphological changes in neuronal cells through the Rho-ROCK pathway (10, 11, 44). It has been proposed that these effects are mediated by LPA<sub>1</sub> and/or LPA<sub>2</sub> (10, 11, 44). Recently, we identified p2y<sub>9</sub>/GPR23 as a fourth LPA receptor (LPA<sub>4</sub>) that is

## LPA<sub>4</sub> Changes the Morphology of Neuronal Cells

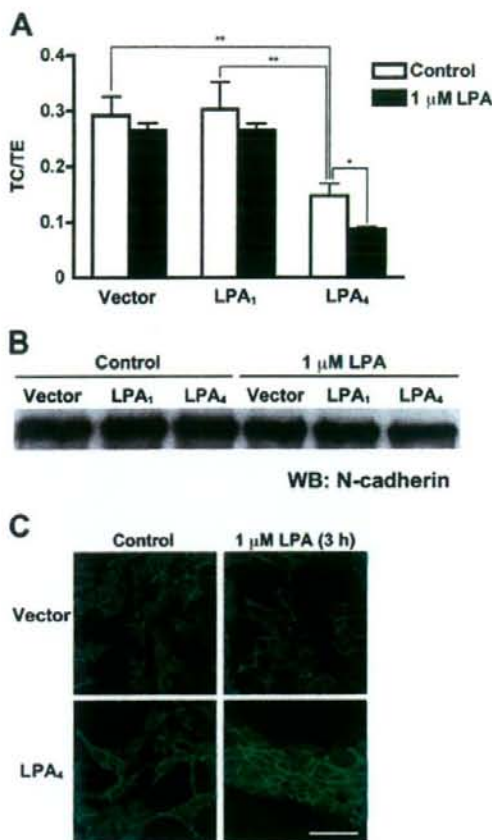


**FIGURE 6. LPA induces N-cadherin-dependent cell adhesion in B103-LPA<sub>4</sub> cells.** A, Ca<sup>2+</sup> dependence of cell-cell adhesion in B103-LPA<sub>4</sub> cells. Serum-starved cells were stimulated with 1 μM LPA for 2 h and washed with HBSS containing either 1 mM Ca<sup>2+</sup> or 1 mM EDTA. The washed cells were treated with 0.01% trypsin for 30 min in the presence of either Ca<sup>2+</sup> (TC treatment) or EDTA (TE treatment) at 37 °C. Then the cells were dissociated by pipetting 10 times, and the number of particles was counted with a particle counter. The degree of cell-cell adhesion was expressed as the ratio of TC/TE. Note that the ratio inversely reflects cadherin activity. Negative control experiments without LPA treatment were also performed. Data are means ± S.E. of five independent experiments. \*, *p* < 0.05; \*\*, *p* < 0.001 (using analysis of variance followed by Tukey-Kramer test). B, expression of N-cadherin protein in B103 cells. Serum-starved cells were incubated with or without 1 μM LPA for 3 h and lysed. The same amount of protein was subjected to Western blot (WB) analysis. C, immunostaining of N-cadherin in B103-vector and B103-LPA<sub>4</sub> cells. Serum-starved cells were stimulated with 1 μM LPA, stained with an antibody against N-cadherin, and visualized with a fluorescein-labeled secondary antibody. Negative control experiments without LPA treatment were also performed. Bar, 100 μm.

structurally distinct from the EDG family of LPA receptors (19). The expression of LPA<sub>4</sub> in neuronal cells implies a significant role for this receptor in the nervous system (18). The results in this study demonstrate that LPA<sub>4</sub> caused morphological changes in B103 neuronal cells, including cell rounding and N-cadherin-associated cell aggregation, both of which were mediated by the Rho-ROCK pathway.

Ca<sup>2+</sup> mobilization and adenylyl cyclase inhibition are the major cellular responses to LPA (45). When expressed in B103



## LPA<sub>4</sub> Changes the Morphology of Neuronal Cells

neuronal cells, each of the EDG family LPA receptors, LPA<sub>1</sub>, LPA<sub>2</sub>, and LPA<sub>3</sub>, mediates both of these reactions (30). LPA<sub>1</sub> is likely to mediate the Ca<sup>2+</sup> response through G<sub>q/11</sub> proteins (Fig. 3). The PTX-sensitive inhibition of adenylyl cyclase (Fig. 2A) suggests that LPA<sub>1</sub> also couples to G<sub>i/o</sub>. We showed that LPA<sub>4</sub> mediates the Ca<sup>2+</sup> response in B103 cells (Fig. 3). This is consistent with our previous report (19) that the stable expression of LPA<sub>4</sub> in Chinese hamster ovary cells significantly enhanced the LPA-induced Ca<sup>2+</sup> mobilization. From our results using YM-254890, LPA<sub>4</sub> probably mediates Ca<sup>2+</sup> mobilization through G<sub>q/11</sub> proteins (Fig. 3). In contrast, LPA did not inhibit adenylyl cyclase in B103-LPA<sub>4</sub> cells (Fig. 2A). These results indicate that unlike the other LPA receptor subtypes, LPA<sub>4</sub> does not couple to G<sub>i/o</sub> proteins.

Neurite retraction and neurite formation play a role in the remodeling of neurons for guidance and synaptic plasticity (46). Neurite retraction in neuronal cells is induced by lysophospholipids, including LPA and sphingosine 1-phosphate (S1P), in addition to semaphorins, netrins, and ephrins (10, 11, 47). LPA induces neurite retraction through LPA<sub>1</sub> or LPA<sub>2</sub> when expressed in B103 cells (30). In this study, we showed that 1 μM LPA induced cell rounding in B103-LPA<sub>4</sub> cells (Fig. 4A). Sugiura *et al.* (48) reported that rat brain contains 3.73 nmol of LPA/g of tissue. These results suggest a role for LPA<sub>4</sub> in LPA-induced neurite retraction. Neurite initiation and formation involve actin cytoskeletal changes, and as a regulator of actin reorganization, Rho GTPase has a profound effect on neurogenesis (47). For example, S1P induces Rho-dependent neurite retraction through the S1P<sub>2</sub> (49, 50), S1P<sub>3</sub> (49), and S1P<sub>5</sub> receptors (50, 51). Several studies have also revealed a critical role for Rho and ROCK in LPA-induced neurite retraction (36, 52, 53), although some studies have reported Rho-independent neurite retraction (38, 54). Judging from its complete inhibition by C3 exoenzyme and Y-27632, the cell rounding induced by LPA<sub>4</sub> depended on Rho and ROCK in B103-LPA<sub>4</sub> cells (Fig. 4, B and C).

In general, activation of G<sub>12/13</sub> proteins leads to an increase in RhoA guanine nucleotide exchange, activation of ROCK, and actin polymerization (55, 56), although some studies have implied that G<sub>q/11</sub> proteins can also activate Rho (57, 58). Based on our results, it is conceivable that the G<sub>12/13</sub> proteins are upstream regulators of Rho in B103-LPA<sub>1</sub> cells and B103-LPA<sub>4</sub> cells, because YM-254890 inhibited cell rounding in both cell types (Fig. 4B). In many studies reporting the induction of neurite retraction by LPA (10), the LPA receptor subtypes responsible have not been identified, or LPA<sub>1</sub> and LPA<sub>2</sub> were suggested as candidate subtypes based on mRNA expression in the neuronal cells examined (59–62). This study suggests the possibility that LPA<sub>4</sub> was involved in the neurite retraction in some of these studies.

LPA has been shown to stimulate cell motility and to modulate tumor cell invasion, both of which are mediated mainly by LPA<sub>1</sub> and G<sub>i/o</sub> proteins (33, 63, 64). In the presence of serum, B103-LPA<sub>1</sub> cells exhibited a flattened morphology and were widely dispersed throughout the dish (Fig. 1B) (33). This morphological phenotype was probably evoked by LPA through the LPA<sub>1</sub>-G<sub>i/o</sub>-Rac signaling axis (33). In sharp contrast to B103-LPA<sub>1</sub> cells, B103-LPA<sub>4</sub> cells formed cell aggregates in serum-

containing medium (Fig. 1B), apparently through activation of the G<sub>12/13</sub>-Rho-ROCK signaling axis (Fig. 5). This cell-cell adhesion involved N-cadherin without *de novo* synthesis (Fig. 6). Because Rho affects cadherin-dependent adhesion through actin cytoskeleton reorganization (28), we presume that LPA-induced cytoskeletal changes affect the subcellular distribution of N-cadherin, as shown in Fig. 6C, leading to strong cell-cell adhesion in B103-LPA<sub>4</sub> cells. This is supported by the current results that treatment with Y-27632 and cytochalasin D abolished the LPA-induced cell aggregation (Fig. 5 and data not shown). N-cadherin is widely expressed in the nervous system and has critical roles in neural development and functions, including synapse formation and myelination. Weiner *et al.* (65) previously reported that LPA induced cell-cell junctions containing N-cadherin in rat Schwann cells. Furthermore, LPA was reported to induce cell clustering in neural progenitor cells prepared from embryonic rat hippocampus (66) and in mouse postmitotic cortical neurons (16). Our results raise the possibility that in addition to LPA<sub>1</sub> and LPA<sub>2</sub>, LPA<sub>4</sub> might also be involved in these effects in neural cells and have critical roles in the development and function of the nervous system. In contrast to LPA<sub>1</sub> and LPA<sub>2</sub>, which activate Rac through G<sub>i/o</sub> (17, 64), LPA<sub>4</sub> is unlikely to activate the G<sub>i/o</sub>-Rac pathway because LPA<sub>4</sub> did not inhibit adenylyl cyclase activity (Fig. 3A). Therefore, LPA<sub>4</sub> might have a unique role in keeping a proper balance between Rho and Rac activation, which is important for neuronal development and function (47).

We observed that PTX significantly enhanced the intensity of LPA<sub>1</sub>-mediated cell rounding (Fig. 4B). This "permissive effect" is consistent with a previous report that PTX enables LPA-induced cell rounding in 1321N1 astrocytoma cells (61). It is known that Rho activity is inhibited by Rac activation through G<sub>i/o</sub> proteins (67). Indeed, Rac activation functionally antagonizes Rho-mediated neurite retraction in 1321N1 astrocytoma cells (61). LPA<sub>1</sub> was shown to couple to G<sub>i/o</sub> and activate Rac strongly in B103 cells (33) and other cells, including mouse embryonic meningeal fibroblast (MEMF) and mouse skin fibroblast (MSF) cells (17, 64). Taken together, we suggest that PTX treatment of B103-LPA<sub>1</sub> cells suppresses G<sub>i/o</sub> proteins and subsequently suppresses Rac activation by LPA, which in turn permits Rho-mediated cell rounding. This mechanism probably also accounts for the LPA-induced aggregation of PTX-treated B103-LPA<sub>1</sub> cells (Fig. 5, A, panel h, and B).

We showed here that LPA<sub>4</sub> has Rho-dependent morphological effects. It has been reported that LPA-induced Rho activation is mediated by LPA<sub>1</sub> and/or LPA<sub>2</sub>. However, pathways independent of LPA<sub>1</sub> and LPA<sub>2</sub> have also been proposed. Contos *et al.* (17) showed that MEMF cells from LPA<sub>1</sub> and LPA<sub>2</sub> double knockouts remained capable of forming stress fibers in response to LPA. This study proposed the presence of unknown LPA receptors in MEMF cells because of the absence of LPA<sub>3</sub> mRNA. Consistent with this, Hama *et al.* (64) reported that LPA activates Rho in MSF cells from LPA<sub>1</sub> and LPA<sub>2</sub> double knockouts. Our results, together with the abundant expression of LPA<sub>4</sub> in MSF cells (64), suggest that LPA<sub>4</sub> may also be involved in LPA-induced Rho activation in these cells. Furthermore, Hama *et al.* (64) observed that Rac activation was totally

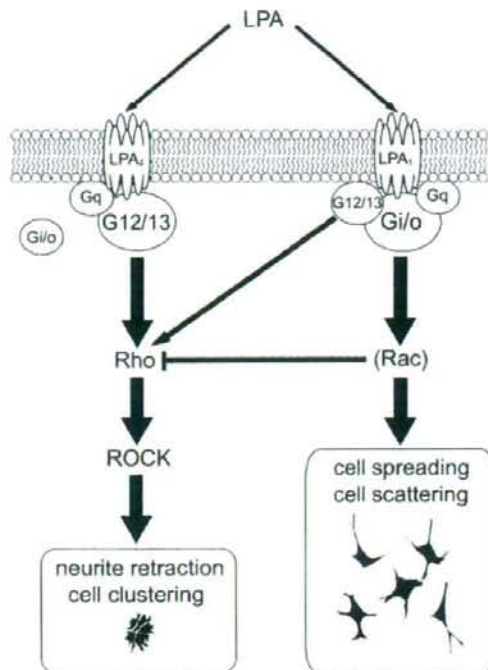


**FIGURE 7. LPA<sub>1</sub> and LPA<sub>4</sub> have distinct signaling pathways that produce different cell morphologies in B103 cells.** LPA<sub>1</sub> expression results in cell rounding and aggregated morphology through G<sub>12/13</sub>-Rho-ROCK pathway. In contrast, LPA<sub>4</sub> expression results in flattened and dispersed morphology as reported previously (33). Inactivation of G<sub>i/o</sub> proteins in LPA<sub>4</sub>-expressing cells by PTX treatment leads to "LPA<sub>4</sub>-expressing cells like" aggregated morphology, suggesting the involvement of the inhibitory effect of G<sub>i/o</sub> on Rho activation probably through Rac. Both LPA<sub>1</sub> and LPA<sub>4</sub> couple to G<sub>q</sub>, although G<sub>q</sub>-involved pathway does not affect cell morphology.

dependent on LPA<sub>1</sub> and LPA<sub>2</sub>, supporting our hypothesis that LPA<sub>4</sub> does not activate the G<sub>i/o</sub>-Rac signaling axis.

We also observed that the stable expression of LPA<sub>1</sub> or LPA<sub>4</sub> slightly increased the population of rounded cells even before LPA application (Fig. 4B). Furthermore, serum-starved B103-LPA<sub>4</sub> cells adhered to one another more strongly than B103-vector or B103-LPA<sub>1</sub> cells did (Fig. 6A). These morphological effects might be because of the constitutive activation of these LPA receptors. Indeed, there are many reports showing that the constitutive expression of GPCR for lipid mediators, including lysophospholipids and prostanoids, has morphological effects (30, 49, 68, 69). For example, cell rounding and cadherin-dependent adhesion in the absence of ligand occur in human embryonic kidney 293 cells transfected with FP<sub>B</sub> receptor, an isoform of prostanoid GPCR (69, 70). The involvement of phosphatidylinositol 3-kinase and  $\beta$ -catenin was proposed for these constitutive activities (70). Another conceivable explanation for the morphological effects observed in serum-starved B103-LPA<sub>1</sub> and B103-LPA<sub>4</sub> cells involves autocrine ligand secretion and subsequent receptor activation (33). Both hypotheses are consistent with our results that the treatment of these cells with Y-27632 decreased the percentage of rounded cells (Fig. 4B).

## LPA<sub>4</sub> Changes the Morphology of Neuronal Cells

In summary, as shown in Fig. 7, we demonstrate for the first time that the novel LPA receptor subtype LPA<sub>4</sub> is coupled to the activation of Rho in a rat neuronal cell line. The activation of Rho through LPA<sub>4</sub> leads to morphological changes, including cell rounding and cell aggregation. LPA is well known to induce neurite retraction and cell clustering in neural cells. The identification of Rho as an effector of LPA<sub>4</sub> will give insight into some of the physiological and morphological effects of LPA that could not be explained by the EDG family LPA receptors. A full understanding of the potential roles of the endogenous LPA<sub>4</sub> receptor in the development and function of the nervous system awaits future studies.

**Acknowledgments**—We thank Drs. T. Yokomizo and T. Okuno (Kyushu University) for vital discussions and critical suggestions. We also thank Dr. J. Chun (The Scripps Research Institute, La Jolla, CA) for providing B103 rat neuroblastoma cells; Dr. J. Miyazaki (Osaka University) for pCXN2; Drs. S. Narumiya (Kyoto University) and S. Nagata (Osaka University) for the expression vector for C3 exoenzyme (pEF-C3) and its parental vector (pEF-BOS), respectively; and Dr. J. Takasaki (Astellas Pharma, Tokyo, Japan) for YM-254890.

## REFERENCES

- Moolenaar, W. H., van Meeteren, L. A., and Giepmans, B. N. (2004) *BioEssays* **26**, 870–881
- Anliker, B., and Chun, J. (2004) *J. Biol. Chem.* **279**, 20555–20558
- Hecht, J. H., Weiner, J. A., Post, S. R., and Chun, J. (1996) *J. Cell Biol.* **135**, 1071–1083
- An, S., Bicu, T., Zhong, Y., and Goetzl, E. J. (1998) *Mol. Pharmacol.* **54**, 881–888
- Bandoh, K., Aoki, J., Hosono, H., Kobayashi, S., Kobayashi, T., Murakami-Murofushi, K., Tsujimoto, M., Arai, H., and Inoue, K. (1999) *J. Biol. Chem.* **274**, 27776–27785
- Contos, J. J., Ishii, I., and Chun, J. (2000) *Mol. Pharmacol.* **58**, 1188–1196
- Ishii, I., Fukushima, N., Ye, X., and Chun, J. (2004) *Annu. Rev. Biochem.* **73**, 321–354
- Das, A. K., and Hajra, A. K. (1989) *Lipids* **24**, 329–333
- Tokumura, A. (1995) *Prog. Lipid Res.* **34**, 151–184
- Ye, X., Fukushima, N., Kingsbury, M. A., and Chun, J. (2002) *Neuroreport* **13**, 2169–2175
- Chun, J. (2005) *Prostaglandins Other Lipid Mediat.* **77**, 46–51
- Contos, J. J., Fukushima, N., Weiner, J. A., Kaushal, D., and Chun, J. (2000) *Proc. Natl. Acad. Sci. U. S. A.* **97**, 13384–13389
- Harrison, S. M., Reavill, C., Brown, G., Brown, J. T., Cluderay, J. E., Crook, B., Davies, C. H., Dawson, L. A., Grau, E., Heidbreder, C., Hemmati, P., Hervieu, G., Howarth, A., Hughes, Z. A., Hunter, A. J., Latham, J., Pickering, S., Pugh, P., Rogers, D. C., Shilliam, C. S., and Maycox, P. R. (2003) *Mol. Cell. Neurosci.* **24**, 1170–1179
- Inoue, M., Rashid, M. H., Fujita, R., Contos, J. J., Chun, J., and Ueda, H. (2004) *Nat. Med.* **10**, 712–718
- Kingsbury, M. A., Rehen, S. K., Contos, J. J., Higgins, C. M., and Chun, J. (2003) *Nat. Neurosci.* **6**, 1292–1299
- Fukushima, N., Weiner, J. A., Kaushal, D., Contos, J. J., Rehen, S. K., Kingsbury, M. A., Kim, K. Y., and Chun, J. (2002) *Mol. Cell. Neurosci.* **20**, 271–282
- Contos, J. J., Ishii, I., Fukushima, N., Kingsbury, M. A., Ye, X., Kawamura, S., Brown, J. H., and Chun, J. (2002) *Mol. Cell. Biol.* **22**, 6921–6929
- Jin Rhee, H., Nam, J. S., Sun, Y., Kim, M. J., Choi, H. K., Han, D. H., Kim, N. H., and Huh, S. O. (2006) *Neuroreport* **17**, 523–526
- Noguchi, K., Ishii, S., and Shimizu, T. (2003) *J. Biol. Chem.* **278**, 25600–25606
- Janssens, R., Boeynaems, J. M., Godart, M., and Communi, D. (1997) *Biochem. Biophys. Res. Commun.* **236**, 106–112
- O'Dowd, B. F., Nguyen, T., Jung, B. P., Marchese, A., Cheng, R., Heng, H. H., Kolakowski, L. F., Jr., Lynch, K. R., and George, S. R. (1997) *Gene*

## LPA<sub>4</sub> Changes the Morphology of Neuronal Cells

- (*Amst.*) 187, 75–81
22. Fujiwara, Y., Sebok, A., Meakin, S., Kobayashi, T., Murakami-Murofushi, K., and Tigyi, G. (2003) *J. Neurochem.* 87, 1272–1283
  23. Takasaki, J., Saito, T., Taniguchi, M., Kawasaki, T., Moritani, Y., Hayashi, K., and Kobori, M. (2004) *J. Biol. Chem.* 279, 47438–47445
  24. Niwa, H., Yamamura, K., and Miyazaki, J. (1991) *Gene (Amst.)* 108, 193–199
  25. Fujisawa, K., Madaule, P., Ishizaki, T., Watanabe, G., Bito, H., Salto, Y., Hall, A., and Narumiya, S. (1998) *J. Biol. Chem.* 273, 18943–18949
  26. Mizushima, S., and Nagata, S. (1990) *Nucleic Acids Res.* 18, 5322
  27. Nagafuchi, A., Ishihara, S., and Tsukita, S. (1994) *J. Cell Biol.* 127, 235–245
  28. Fukata, M., Kuroda, S., Nakagawa, M., Kawajiri, A., Itoh, N., Shoji, I., Matsuura, Y., Yonehara, S., Fujisawa, H., Kikuchi, A., and Kaibuchi, K. (1999) *J. Biol. Chem.* 274, 26044–26050
  29. Fukushima, N., Kimura, Y., and Chun, J. (1998) *Proc. Natl. Acad. Sci. U. S. A.* 95, 6151–6156
  30. Ishii, L., Contos, J. J., Fukushima, N., and Chun, J. (2000) *Mol. Pharmacol.* 58, 895–902
  31. Tsukahara, T., Tsukahara, R., Yasuda, S., Makarova, N., Valentine, W. J., Allison, P., Yuan, H., Baker, D. L., Li, Z., Bittman, R., Parrill, A., and Tigyi, G. (2006) *J. Biol. Chem.* 281, 3398–3407
  32. Bockaert, J., and Pin, J. P. (1999) *EMBO J.* 18, 1723–1729
  33. van Leeuwen, F. N., Olivo, C., Grivell, S., Giepmans, B. N., Collard, I. G., and Moolenaar, W. H. (2003) *J. Biol. Chem.* 278, 400–406
  34. Meyer Zu Heringdorf, D. (2004) *J. Cell. Biochem.* 92, 937–948
  35. von Kugelgen, I. (2006) *Pharmacol. Ther.* 110, 415–432
  36. Jalink, K., van Corven, E. J., Hengeveld, T., Morii, N., Narumiya, S., and Moolenaar, W. H. (1994) *J. Cell Biol.* 126, 801–810
  37. Katoh, H., Aoki, J., Yamaguchi, Y., Kitano, Y., Ichikawa, A., and Negishi, M. (1998) *J. Biol. Chem.* 273, 28700–28707
  38. Couvillon, A. D., and Exton, J. H. (2006) *Cell. Signal.* 18, 715–728
  39. Hall, A. (1998) *Science* 279, 509–514
  40. Takeichi, M. (1977) *J. Cell Biol.* 75, 464–474
  41. Gumbiner, B. M. (2005) *Nat. Rev. Mol. Cell Biol.* 6, 622–634
  42. Chen, Q., Chen, T. J., Letourneau, P. C., Costa Lda, F., and Schubert, D. (2005) *J. Neurosci.* 25, 281–290
  43. Wanner, I. B., and Wood, P. M. (2002) *J. Neurosci.* 22, 4066–4079
  44. Fukushima, N. (2004) *J. Cell. Biochem.* 92, 993–1003
  45. Tigyi, G. (2001) *Prostaglandins Other Lipid Mediat.* 64, 47–62
  46. Luo, L., and O'Leary, D. D. (2005) *Annu. Rev. Neurosci.* 28, 127–156
  47. Govek, E. E., Newey, S. E., and Van Aelst, L. (2005) *Genes Dev.* 19, 1–49
  48. Sugiura, T., Nakane, S., Kishimoto, S., Waku, K., Yoshioka, Y., Tokumura, A., and Hanahan, D. J. (1999) *Biochim. Biophys. Acta* 1440, 194–204
  49. van Brocklyn, J. R., Tu, Z., Edsall, L. C., Schmidt, R. R., and Spiegel, S. (1999) *J. Biol. Chem.* 274, 4626–4632
  50. Toman, R. E., Payne, S. G., Watterson, K. R., Maceyka, M., Lee, N. H., Milstien, S., Bigbee, J. W., and Spiegel, S. (2004) *J. Cell Biol.* 166, 381–392
  51. Jaillard, C., Harrison, S., Stankoff, B., Aigrot, M. S., Calver, A. R., Duddy, G., Walsh, F. S., Pangalos, M. N., Arimura, N., Kaibuchi, K., Zalc, B., and Lubetzk, C. (2005) *J. Neurosci.* 25, 1459–1469
  52. Hirose, M., Ishizaki, T., Watanabe, N., Uehata, M., Kranenburg, O., Moolenaar, W. H., Matsumura, F., Maekawa, M., Bito, H., and Narumiya, S. (1998) *J. Cell Biol.* 141, 1625–1636
  53. Kranenburg, O., Poland, M., van Horck, F. P., Drechsel, D., Hall, A., and Moolenaar, W. H. (1999) *Mol. Biol. Cell* 10, 1851–1857
  54. Somlyo, A. P., and Somlyo, A. V. (2000) *J. Physiol. (Lond.)* 522, 177–185
  55. Hart, M. J., Jiang, X., Kozasa, T., Roscoe, W., Singer, W. D., Gilman, A. G., Sternweis, P. C., and Bollag, G. (1998) *Science* 280, 2112–2114
  56. Kozasa, T., Jiang, X., Hart, M. J., Sternweis, P. M., Singer, W. D., Gilman, A. G., Bollag, G., and Sternweis, P. C. (1998) *Science* 280, 2109–2111
  57. Chikumi, H., Vazquez-Prado, J., Servitja, J. M., Miyazaki, H., and Gutkind, J. S. (2002) *J. Biol. Chem.* 277, 27130–27134
  58. Vogt, S., Grosse, R., Schultz, G., and Offermanns, S. (2003) *J. Biol. Chem.* 278, 28743–28749
  59. Sayas, C. L., Avila, J., and Wandosell, F. (2002) *J. Neurosci.* 22, 6863–6875
  60. Dawson, J., Hotchin, N., Lax, S., and Rumsby, M. (2003) *J. Neurochem.* 87, 947–957
  61. Seaholtz, T. M., Radeff-Huang, J., Sagi, S. A., Matteo, R., Weems, J. M., Cohen, A. S., Feramisco, J. R., and Brown, J. H. (2004) *J. Neurochem.* 91, 501–512
  62. Sayas, C. L., Moreno-Flores, M. T., Avila, J., and Wandosell, F. (1999) *J. Biol. Chem.* 274, 37046–37052
  63. Yamada, T., Sato, K., Komachi, M., Malchinkhuu, E., Toba, M., Kimura, T., Kuwabara, A., Yanagita, Y., Ikeya, T., Tanahashi, Y., Ogawa, T., Ohwada, S., Morishita, Y., Ohta, H., Im, D. S., Tamoto, K., Tomura, H., and Okajima, F. (2004) *J. Biol. Chem.* 279, 6595–6605
  64. Hama, K., Aoki, J., Fukaya, M., Kishi, Y., Sakai, T., Suzuki, R., Ohta, H., Yamori, T., Watanabe, M., Chun, J., and Arai, H. (2004) *J. Biol. Chem.* 279, 17634–17639
  65. Weiner, J. A., Fukushima, N., Contos, J. J., Scherer, S. S., and Chun, J. (2001) *J. Neurosci.* 21, 7069–7078
  66. Harada, J., Foley, M., Moskowitz, M. A., and Waerber, C. (2004) *J. Neurochem.* 88, 1026–1039
  67. Burrige, K., and Wennerberg, K. (2004) *Cell* 116, 167–179
  68. Hasegawa, H., Negishi, M., Katoh, H., and Ichikawa, A. (1997) *Biochem. Biophys. Res. Commun.* 234, 631–636
  69. Pierce, K. L., Fujino, H., Srinivasan, D., and Regan, J. W. (1999) *J. Biol. Chem.* 274, 35944–35949
  70. Fujino, H., Srinivasan, D., and Regan, J. W. (2002) *J. Biol. Chem.* 277, 48786–48795

# Eosinophil Trans-Basement Membrane Migration Induced by Interleukin-8 and Neutrophils

Izumi Kikuchi, Shinya Kikuchi, Takehito Kobayashi, Koichi Hagiwara, Yoshio Sakamoto, Minoru Kanazawa, and Makoto Nagata

Department of Respiratory Medicine, Saitama Medical School, Saitama, Japan; and Department of Allergy and Respiratory Medicine, Kanto Central Hospital of the Mutual Aid Association of Public School Teachers, Tokyo, Japan

Neutrophilic inflammation observed with severe asthma is often associated with interleukin-8 (IL-8). Neutrophils can secrete a variety of mediators that may augment the migration of eosinophils. We have reported a positive correlation between the concentrations of neutrophils and eosinophils in sputum from subjects with severe asthma, suggesting a possible role of neutrophils in regulating eosinophilic inflammation. The aim of this study was to investigate whether neutrophils stimulated with IL-8 modify the trans-basement membrane migration (TBM) of eosinophils. Eosinophils and neutrophils were isolated from peripheral blood drawn from healthy donors or subjects with mild asthma. The TBM of eosinophils in response to IL-8 was evaluated in the presence or absence of neutrophils using the chambers with a Matrigel-coated transwell insert. Neither IL-8 alone nor the presence of neutrophils alone induced the TBM of eosinophils. However, when eosinophils were cocultured with neutrophils and stimulated with IL-8, the TBM of eosinophils was significantly augmented. This augmented TBM of eosinophils was inhibited by a matrix metalloproteinase-9 inhibitor, a leukotriene B<sub>4</sub> receptor antagonist, platelet-activating factor antagonists, or an anti-TNF- $\alpha$  monoclonal antibodies. These results suggest that neutrophils migrated in response to IL-8 may lead eosinophils to accumulate in the airways of asthma and possibly aggravate this disease.

**Keywords:** eosinophils; growth-related oncogene- $\alpha$ ; interleukin-8; neutrophils; trans-basement membrane migration

Eosinophils, inflammatory cells predominantly found in the airways of patients with asthma, likely contribute to airway remodeling or airflow limitation observed with asthma (1–4). The mechanism by which eosinophils accumulate in the airways is a complex process that is mainly regulated by cytokines, chemokines, and adhesion molecules. This process is likely to be inhibited by corticosteroid treatment via the suppression of cytokines/chemokines productions from corticosteroid-sensitive cells such as Th2 cells. In a subgroup of patients, accumulation of neutrophils is found in their airways even in the absence of apparent infection. Asthma in such patients is often severe and chronic and is refractory to corticosteroid therapy (5–8). Based on a recent report from the European network study for understanding mechanisms of severe asthma (ENFUMOSA), patients with severe asthma have greater sputum neutrophilia and evidence of ongoing eosinophil-derived mediator release, compared with patients with mild to moderate asthma, suggesting that both neutrophilic and eosinophilic inflammation persists in the airways of severe asthma (9). In this context, we have recently reported a positive correlation between the concentrations of

neutrophils and eosinophils in induced sputum from patients with severe persistent asthma who are treated with medicines including systemic corticosteroid (10).

Functions of neutrophils are not effectively suppressed by corticosteroids (11, 12), suggesting that neutrophils may play a role in the pathophysiology of the disease in such patients. There are many reports which suggest that neutrophils are exposed to a variety of inflammatory mediators in the airways of patients with asthma. For example, interleukin-8 (IL-8), which acts as a chemoattractant for neutrophils, is found in bronchoalveolar lavage fluid and serum from patients with asthma (13–16). Concentration of IL-8 has been shown to be correlated with accumulation of neutrophils in the airways of asthma (6), and therefore this chemokine may be an essential molecule responsible for the development of neutrophilic inflammation in asthma. Activated neutrophils can secrete a variety of mediators (e.g., matrix metalloproteinases [MMPs], leukotriene B<sub>4</sub> [LTB<sub>4</sub>], platelet-activating factor [PAF], and TNF- $\alpha$ ) that can induce digestion of basement membrane, or migration or activation of eosinophils (17, 18), and may thus contribute to the pathophysiology of asthma.

We framed a hypothesis that neutrophils stimulated with and migrated to IL-8 play roles in the regulation of eosinophilic inflammation in asthma. Trans-basement membrane migration (TBM) is one of the key processes by which circulating eosinophils accumulate in the airways of asthma. Here we report that a combination of IL-8 and neutrophils augment the TBM of eosinophils.

## MATERIALS AND METHODS

### Reagents

Anti-CD16 antibody-coated magnetic beads were purchased from Miltenyi Biotec (Auburn, CA). Percoll was purchased from Pharmacia (Uppsala, Sweden). HBSS was purchased from GIBCO BRL (Grand Island, NY). BIL260, an LTB<sub>4</sub> receptor antagonist, and WEB2086 and WEB2170, PAF receptor antagonists, were provided by Boehringer Ingelheim (Ridgefield, CT). MMP-9 inhibitor and GM1489, an MMP inhibitor, was purchased from Calbiochem (San Diego, CA). AA861, a 5-lipoxygenase (LO) inhibitor, and PBS were obtained from Wako (Osaka, Japan). IL-8, Growth-related oncogene- $\alpha$  (GRO- $\alpha$ ), TNF- $\alpha$ , eotaxin, regulated upon activation, normal T cell expressed and secreted (RANTES), and anti-CXC chemokine receptor 2 (CXCR2) antibody were purchased from R&D Systems (Minneapolis, MN). LTB<sub>4</sub> was purchased from Cayman Chemical (Ann Arbor, MI). PAF, Phorbol 12-myristate 13-acetate (PMA),  $\alpha$ -phenylethylamine (OPD), and BSA were obtained from Sigma (St. Louis, MO). Anti-TNF- $\alpha$  monoclonal antibody (mAb) (clone Mab11, mouse IgG1) was purchased from Becton Dickinson (Franklin Lakes, NJ). Mouse IgG1, an isotype control for anti-TNF- $\alpha$  mAb, and newborn calf serum (NCS) were purchased from ICN Biomedicals, Inc. (Aurora, OH). The acetoxy methyl ester of 2'-7'-bis (2-carboxy-ethyl)-5(6)-carboxyfluorescein (BCECF-AM) was purchased from Dojin Laboratory (Kumamoto, Japan).

### Preparation of Neutrophils and Eosinophils

Neutrophils and eosinophils were isolated from peripheral blood collected from nonatopic healthy donors whose eosinophil content was < 5% of

(Received in original form August 4, 2005 and in final form January 18, 2006)

Correspondence and requests for reprints should be addressed to Makoto Nagata M.D., Ph.D., Department of Respiratory Medicine, Saitama Medical School, Saitama, Japan. E-mail: favre4mn@saitama-med.ac.jp

Am J Respir Cell Mol Biol Vol 34, pp 390–395, 2006

Originally Published in Press as DOI: 10.1165/rcmb.2005-0303OC on February 2, 2006  
Internet address: www.atsjournals.org

their peripheral leukocytes. In some experiments, cells isolated from individuals with mild intermittent asthma were also used. The numbers of males and females were comparable among donors, with similar age distributions ranging from 20–38 yr. Informed consent was obtained before collection of each blood sample. Neutrophils and eosinophils were separated by the combination of Percoll density gradient centrifugation and negative immunomagnetic bead selection as previously described (19, 20). Briefly, 40 ml of dextran were added to 160 ml of heparinized blood, and erythrocytes were removed as sediment. The remaining suspension of leukocytes was layered onto Percoll gradients of 1.080, 1.085, and 1.090 g/ml in density. After centrifugation at  $700 \times g$  for 20 min, neutrophils (purity exceeded 95%) were collected from 1.085/1.090 g/ml interface, and suspended in HBSS containing 0.2% BSA (HBSS/BSA buffer). After the removal of Percoll, the red blood cells in the pellet were lysed by hypotonic shock and removed by washing with cold PBS. The remaining cells were washed with 4°C HBSS supplemented with 2% NCS (HBSS/NCS), then incubated with anti-CD16 antibody-coated magnetic beads for 30 min at 4°C, and were then filtered with a column containing steel wool placed in a magnetic field (Miltenyi Biotec). Eosinophils (>98% purity and >99% viability), which passed through the column, were collected and washed, and the number of cells was adjusted to  $2.5 \times 10^5$  cells/ml by using HBSS/BSA buffer.

### TBM

The TBM of neutrophils and eosinophils was examined using a modified Boyden's chamber method (21). The study was conducted in duplicate. Briefly, neutrophils were suspended in loading buffer with BCECF-AM at a final concentration of 1  $\mu$ M and incubated for 30 min at 37°C while shading the light (22, 23). The cells retain the label at least for 90 min (23) and superoxide anion generation in response to PMA (0.5 ng/ml) was not modified by BCECF-AM (our unpublished observation). Labeled neutrophils ( $0.5 \times 10^5$  cells), eosinophils ( $0.5 \times 10^5$  cells), or a combination thereof ( $0.5 \times 10^5$  cells plus  $0.5 \times 10^5$  cells) in a 200- $\mu$ l medium were added to the upper compartment of a chamber with a Matrigel-coated transwell insert (pore size 3  $\mu$ m; Becton Dickinson Labware). Either the control medium (500  $\mu$ l) or a medium that contained one of activators (IL-8, GRO- $\alpha$ , eotaxin, RANTES, and LTB $_4$ ) was added to the lower compartment of the chamber. After a 2-h incubation in 5% CO $_2$  at 37°C, the medium in the upper compartment of the chamber and the inserts between the chambers were gently removed. The peroxidase activity of eosinophils in the medium in the lower compartment of the chamber was determined, and the number of migrated eosinophils was calculated from the activity of the standard media which contained known numbers ( $5 \times 10^3$ ,  $1.5 \times 10^4$ ,  $5 \times 10^4$ ,  $1.5 \times 10^5$ , and  $5 \times 10^5$  cells) of eosinophils. To determine the peroxidase activity of eosinophils, the medium was incubated with a substrate (1 mM OPD, 1 mM H $_2$ O $_2$ , and 0.1% Triton X-100 in Tris-HCl, pH 8.0) for 30 min at room temperature (21). The reaction was stopped by adding 100  $\mu$ l of 4N H $_2$ SO $_4$ , and absorbance at 490 nm was determined (21). The effect of neutrophils on the outer density value in this assay was negligible:  $0.046 \pm 0.002$  for 0% control and  $0.064 \pm 0.006$  for 100% control of neutrophils, respectively ( $n = 4$ ). Similarly, addition of neutrophils to 100% control of eosinophils did not modify the outer density value ( $1.566 \pm 0.023$  by addition of 0% control versus  $1.569 \pm 0.012$  by addition of 100% control of neutrophils ( $n = 4$ ,  $P = n.s.$ ). The numbers of migrated neutrophils were determined by the measurement of fluorescence in the medium using the Fluoromark (Bio-Rad Laboratories, Hercules, CA) microplate fluorometer (23). The number of migrated neutrophils determined by this method was highly correlated with those counted by hemocytometer ( $n = 13$ ,  $P < 0.001$ ,  $r = 0.9$ , Pearson's correlation coefficient). The viability of both eosinophils and neutrophils after migration exceeded 98% by trypan blue exclusion.

### Blocking Study

Both eosinophils and neutrophils were incubated in a medium containing Biil260, WEB2086, WEB2170 or AA861 for 15 min at 37°C, in a medium containing anti-TNF- $\alpha$  mAb (clone Mab11) or an isotype matched control mouse IgG1 for 15 min at ambient temperature, or in a medium containing MMP-9 inhibitor for 30 min at 37°C. The media containing the cells were then transferred to the upper compartment of the chamber, and the assay was performed as described above.

### Statistical Analysis

Values are expressed as means  $\pm$  SEM. Student's  $t$  test was conducted to compare two groups, and repeated-measures ANOVA with Scheffé's constants were used to compare more than two groups. A value of  $P < 0.05$  was considered statistically significant.

## RESULTS

### Effects of Neutrophils on the TBM of Eosinophils

To investigate whether stimulated neutrophils affect the TBM of eosinophils, we cocubated a mixture of eosinophils and neutrophils in the presence or absence of IL-8, a CXC chemokine that selectively stimulates chemotactic response of neutrophils. Preliminary experiments confirmed that 10 nM of IL-8 is sufficient to induce the TBM of neutrophils (data not shown). Neither a cocubation with neutrophils nor IL-8 (10 nM) alone induced the TBM of eosinophils (migrated eosinophils:  $0.9 \pm 0.4\%$  by medium control,  $2.2 \pm 0.8\%$  by cocubation with neutrophils,  $P = n.s.$ ;  $1.9 \pm 0.5\%$  by IL-8 alone,  $P = n.s.$ ;  $n = 10$ ) (Figure 1). However, when eosinophils were cocubated with neutrophils and stimulated with IL-8, a significant TBM of eosinophils was observed (migrated eosinophils:  $12.9 \pm 3.1\%$ ,  $P < 0.01$  versus the other three conditions;  $n = 10$ ) (Figure 1). Checkerboard analysis confirmed that the effect of IL-8 on the TBM of eosinophils cocubated with neutrophils is chemotactic ( $n = 3$ , data not shown). When the transmigrations of neutrophils by IL-8 and eosinophils by a combination of IL-8 and neutrophils were simultaneously examined, the capacity of eosinophils to migrate was significantly correlated with the number of neutrophils that migrate ( $P = 0.002$ ,  $r = 0.54$ ,  $n = 6$ ). The time-course profile of TBM of eosinophils traced that of neutrophils: the TBM of neutrophils reached a plateau within the first 15 min, whereas eosinophil TBM mainly occurs 15–60 min after the initiation of reaction ( $n = 6$ , data not shown). In selected experiments, where the effect of IL-8 and neutrophils on the TBM of eosinophils was examined using both eosinophils and neutrophils from donors with mild asthma provided similar results: only a combination of IL-8 and neutrophils induced the TBM of eosinophils ( $n = 3$ , data not shown). Furthermore, when eosinophils were cocubated with neutrophils from different donors, a similar phenomenon was observed: only a combination of IL-8 and neutrophils, but not IL-8 alone or neutrophils alone, induced the TBM of eosinophils ( $n = 3$ , data not shown). GRO- $\alpha$  (10 nM), another CXC chemokine, showed similar results: the TBM of

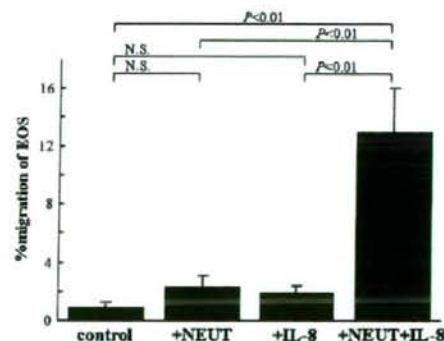


Figure 1. Effects of neutrophils and IL-8 (10 nM) on the TBM of eosinophils. The means  $\pm$  SEM of 10 experiments using cells from different donors are shown. N.S., not significant.

eosinophils was significantly induced only when eosinophils were cocubated with neutrophils and stimulated with GRO- $\alpha$  (migrated eosinophils:  $0.6 \pm 0.3$  by medium control,  $1.2 \pm 0.4$  by a cocubation with neutrophils,  $P = \text{n.s.}$ ;  $0.8 \pm 0.7$  by GRO- $\alpha$  alone,  $P = \text{n.s.}$ ;  $7.1 \pm 2.3$  by a combination of GRO- $\alpha$  and cocubation with neutrophils,  $P < 0.05$  versus the other three conditions,  $n = 4$ ; Figure 2A). LTB $_4$  (100nM), which is chemotactic for both eosinophils and neutrophils, directly induced the TBM of eosinophils; however, the TBM of eosinophils was enhanced when both eosinophils and neutrophils were cocubated (migrated eosinophils:  $1.0 \pm 0.8$  by medium control,  $1.2 \pm 0.9$  by a cocubation with neutrophils,  $P = \text{n.s.}$ ;  $12.9 \pm 4.6$  by LTB $_4$  alone,  $P < 0.05$  versus control;  $23.6 \pm 6.0$  by a combination of LTB $_4$  and cocubation with neutrophils,  $P < 0.05$  versus the other three conditions,  $n = 5$ ; Figure 2B). Finally, eotaxin (3 nM), a CC chemokine that selectively stimulates chemotactic response of eosinophils, induced the TBM of eosinophils (migrated eosinophils:  $2.9 \pm 0.7$  by medium control versus  $59.5 \pm 3.8$  by eotaxin alone,  $P < 0.01$ ). Cocubation with neutrophils did not modify the TBM of eosinophils in response to eotaxin (migrated eosinophils:  $62.3 \pm 4.5$ ,  $P = \text{n.s.}$  versus eotaxin alone,  $n = 5$ ;

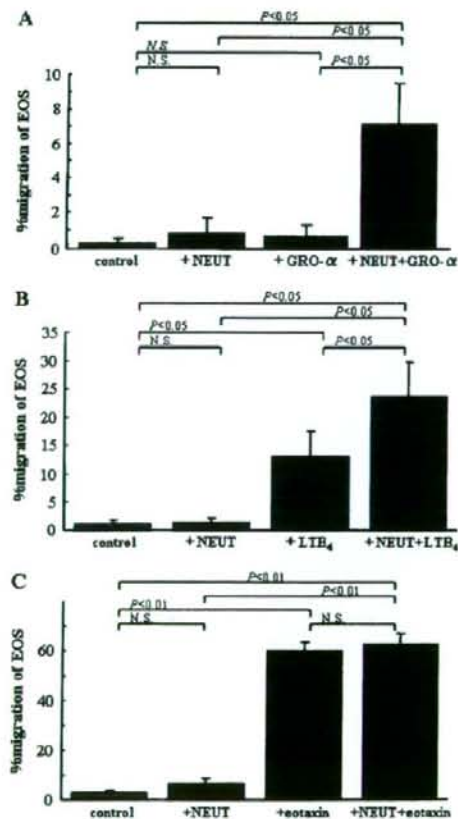


Figure 2. Effects of neutrophils and a variety of agonists on the TBM of eosinophils. Molecules used were GRO- $\alpha$  (10 nM, A), LTB $_4$  (100 nM, B), and eotaxin (10 nM, C). The means  $\pm$  SEM of four to five experiments using cells from different donors are shown. N.S., not significant.

Figure 2C). Similar results were obtained when RANTES, another CC chemokine, was an activator ( $n = 3$ , data not shown).

#### MMP-9, LTB $_4$ , PAF, and TNF- $\alpha$ Are Involved in the Augmentation of Eosinophil TBM by IL-8-Stimulated Neutrophils

The results shown the above sections suggest that neutrophils act as regulators to affect TBM of eosinophils. Suppression of neutrophil-derived protease may lead to the suppression of TBM of eosinophils. To test this hypothesis, we inhibited MMPs, which work when cells digest the basement membrane during intrusion. An MMP-9 inhibitor (10  $\mu$ M) could inhibit the augmented TBM of eosinophils in the presence of IL-8-activated neutrophils (Figure 3A). Similar results were observed when GM1489, an inhibitor of MMPs, was tested ( $n = 5$ , data not shown).

Activated neutrophils may secrete stimulatory molecules for eosinophils and thus augment their TBM as observed above. LTB $_4$ , PAF, and TNF- $\alpha$  are the representative molecules secreted by neutrophils and are capable of activating eosinophils. To investigate whether they are involved, we inhibited the activity of these molecules and observed whether the TBM of eosinophils was suppressed. Reagents used were BIIL260, an LTB $_4$  receptor antagonist; WEB2086, a PAF receptor antagonist; and an anti-TNF- $\alpha$  monoclonal antibody (anti-TNF- $\alpha$  mAb, clone Mab11, mouse IgG1, 3  $\mu$ g/ml). All of these reagents partially suppressed the TBM of eosinophils in the presence of IL-8-activated neutrophils but showed no effect in the absence (Figures 3B–3D). Similar results

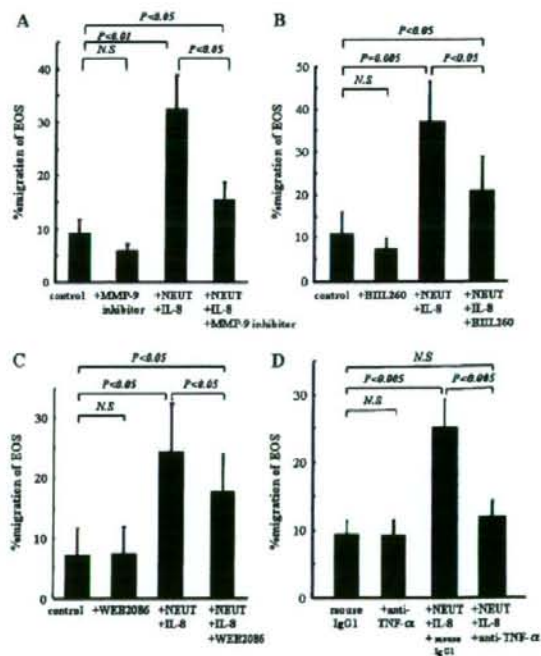


Figure 3. Effects of MMP-9 inhibitor (10  $\mu$ M, A); BIIL260, an LTB $_4$ -antagonist (1  $\mu$ M, B); WEB2086, a PAF-antagonist (10  $\mu$ M, C); and an anti-TNF- $\alpha$  antibody (clone Mab11, isotype mouse IgG1, 3  $\mu$ g/ml; D) on the TBM of eosinophils in the presence of neutrophils stimulated by IL-8. The means  $\pm$  SEM of five to seven experiments using cells from different donors are shown.

were obtained in the studies using AA861, a 5-LO inhibitor that suppresses the production of LTB<sub>4</sub>, and WEB2070, another PAF receptor antagonist (data not shown). These results indicate that the augmentation of eosinophil TBM due to IL-8-stimulated neutrophils is partly mediated by LTB<sub>4</sub>, PAF, and TNF- $\alpha$ . The effects of these inhibitors on TBM of neutrophils alone or eosinophils alone were also examined: IL-8 (10 nM)-induced TBM of neutrophils was not modified by inhibitors for MMP-9, LTB<sub>4</sub>, PAF, or TNF- $\alpha$  ( $n = 6$ ,  $P = n.s.$ , data not shown). Similarly, eotaxin (3 nM)-induced TBM of eosinophils was not modified by inhibitors for MMP-9, LTB<sub>4</sub>, or PAF ( $n = 6$ ,  $P = n.s.$ , data not shown). Anti-TNF- $\alpha$  mAb slightly but significantly reduced eotaxin-induced TBM of eosinophils (migrated eosinophils:  $48.1 \pm 3.5$  by isotype mouse IgG1 versus  $39.3 \pm 2.4$  by eotaxin alone,  $n = 6$ ,  $P = 0.02$ ), suggesting that TNF- $\alpha$  may act as an autocrine activator and partly contribute to the TBM of eosinophils in this system. Finally, pretreatment of only neutrophils, but not eosinophils, with the various inhibitors did not modify the subsequent TBM of eosinophils in the presence of IL-8-activated neutrophils ( $n = 3$ ,  $P = n.s.$ , data not shown).

#### The Conditioned Medium from IL-8-Stimulated Neutrophils Induces the TBM of Eosinophils

To further examine whether the neutrophils transmigrated to IL-8 produce chemoattractants for eosinophils, neutrophils were added to the upper compartment of a chamber with a Matrigel-coated transwell insert and either the control medium or IL-8 (10 nM) was added to the bottom compartment. After a 2-h incubation in 5% CO<sub>2</sub> at 37°C, the bottom compartments were centrifuged at 4°C for 20 min at 700  $\times$   $g$ . The supernatants were gently recovered and then examined for their ability to induce the TBM of eosinophils. The conditioned medium from a combination of IL-8 and neutrophils significantly induced the TBM of eosinophils as compared with the control medium or the condition medium from neutrophils in the absence of IL-8 (migrated eosinophils:  $7.0 \pm 0.6\%$ ,  $P < 0.05$  versus the other two conditions,  $n = 5$ ).

#### Anti-CXCR2 Antibody Does Not Modify the Augmentation of Eosinophil TBM by IL-8-Stimulated Neutrophils

The augmented TBM of eosinophils observed with IL-8-stimulated neutrophils may be a consequence of modification of the CXCR2, an IL-8 ligand, which is expressed on activated eosinophils (24). Although addition of the anti-CXCR2 antibody partly attenuated the TBM of neutrophils in response to IL-8 (% inhibition:  $53.3 \pm 8.6\%$ ,  $n = 5$ ,  $P < 0.01$  versus isotype control), the augmented TBM of eosinophils in the presence of IL-8 and neutrophils was not significantly modified by this antibody ( $n = 5$ ,  $P = n.s.$ , data not shown). An anti-CXCR1 antibody provided similar results ( $n = 2$ , data not shown).

## DISCUSSION

We showed that neutrophils stimulated with chemoattractant such as IL-8 augment the TBM of eosinophils. The reaction kinetics of the augmented TBM of eosinophils traced that of neutrophils. The augmented TBM of eosinophils by a combination of neutrophils and IL-8 was inhibited by an MMP-9 inhibitor, an LTB<sub>4</sub> receptor antagonist, PAF-antagonists, or an anti-TNF- $\alpha$  mAb. LTB<sub>4</sub>, a chemotactic factor for both neutrophils and eosinophils (18, 25), by itself induced the TBM of eosinophils, and this TBM is augmented by the presence of neutrophils. These results provide a mechanism for our previous observation that a positive correlation between the concentrations of neutrophils and eosinophils in sputum from subjects with severe asthma (10), and suggest that neutrophils can regulate the

accumulation of eosinophils through these mechanisms in the airways of asthma.

The mechanism by which neutrophils enhance the TBM of eosinophils is important. We showed that the inhibition of MMP-9 effectively suppresses the augmented TBM of eosinophils. There is evidence that IL-8 stimulates the release of MMP-9 from neutrophils (26). Moreover, the cellular source of MMP-9 may include eosinophils (27). The MMP-9 inhibitor, which is a selective inhibitor of MMP-9 (IC<sub>50</sub> = 5 nM) (28), did not modify the TBM of neutrophils to IL-8 or eosinophils to eotaxin, suggesting that MMP-9 is not required for TBM induced by these ordinary and potent chemoattractants in these experimental conditions. Nonetheless, our results suggest that digestion of membrane by MMP-9 is involved in the mechanisms of augmented TBM of eosinophils induced by IL-8-stimulated neutrophils. The process of TBM of eosinophils would also require the presence of an activator that acts as either chemotactic or chemokinetic for eosinophils. Zurbier and colleagues (29) reported that eosinophil migration across monolayers of lung epithelial cells in response to complement fragment 5a (C5a), but not to RANTES, PAF, or IL-8, was increased in the presence of neutrophils. They explained that neutrophils, but not eosinophils, rapidly inactivated C5a and decreased the activity of C5a that had diffused into the upper compartment, and thereby maintain a proper C5a chemotactic gradient in their trans-epithelial migration model. In contrast, our study suggested that neutrophils enhanced the TBM of eosinophils, at least in part, via the generation of activators for eosinophils: the inhibition of LTB<sub>4</sub>, PAF, or TNF- $\alpha$  actions partially suppressed TBM of eosinophils. In addition to LTB<sub>4</sub>, PAF is a chemotactic factor for both neutrophils and eosinophils (18, 24). The pharmacologic inhibitors may reduce migration of neutrophils and subsequently reduce migration of eosinophils, instead of acting to disrupt the effects of neutrophil-derived mediators on eosinophils. From this point of view, we observed that IL-8-induced TBM of neutrophils in this system was not modified by inhibitors for LTB<sub>4</sub> or PAF. Furthermore, pretreatment of neutrophils with the various inhibitors did not modify the subsequent TBM of eosinophils in the presence of IL-8-activated neutrophils. TNF- $\alpha$  is not a chemotactic agent for neutrophils or eosinophils itself, but has been shown to be an activator for functions of both neutrophils and eosinophils such as adhesion or respiratory burst (25, 30). Our results that TNF- $\alpha$  is involved in the augmented TBM of eosinophils suggest that the activation of effector function(s) of either neutrophils or eosinophils may be sufficient to augment the TBM of eosinophils. We observed that anti-TNF- $\alpha$  mAb slightly but significantly reduced eotaxin-induced TBM of eosinophils, but not IL-8-induced TBM of neutrophils, suggesting some role of this cytokine as an autocrine activator for eosinophil migration in this system.

Increased concentrations of LTB<sub>4</sub> (31, 32), PAF (33), and TNF- $\alpha$  (34) have been reported in the airways of asthma. Our results suggest that neutrophils are activated via a combination of IL-8 and basement membrane and generate these mediators. In this context, we found that the conditioned medium from a combination of IL-8 and neutrophils, but not neutrophils alone or medium alone, induced the TBM of eosinophils, indicating that the neutrophils transmigrated to IL-8 produce chemoattractant(s) that result in subsequent migration of eosinophils. Taken together, the augmented TBM of eosinophils is likely a complex of the effects of both MMP-9, on the basement membrane, and eosinophil activators and chemoattractants such as LTB<sub>4</sub>, PAF, and TNF- $\alpha$ .

Our assay simulates the initial phase of inflammation involving neutrophils and eosinophils, in which cells are stimulated and

migrate out of blood vessels to accumulate at the inflammation site. In the later phase of inflammation, the expression of surface receptors of cells may be modified to become responsive to molecules that they were initially unresponsive. A good example is the expression of CXCR2, an IL-8 ligand, in activated eosinophils (24). The augmented TBM of eosinophils in the presence of IL-8 and neutrophils was not significantly modified by anti-CXCR2 antibody, ensuring in this assay that eosinophils are activated not directly by IL-8 but via the activation of neutrophils. However, this antibody partly attenuates the TBM of neutrophils to IL-8. Similar results were observed with an anti-CXCR1 antibody. These results suggest that migration of neutrophils is not a sole contributing factor for the augmented eosinophil migration. Not only MMP-9 or chemoattractants released from transmigrated neutrophils, but also the eosinophil activators released from neutrophils activated by IL-8 and integrin-mediated signaling before transmigration, may be important in the subsequent migration of eosinophils. We speculated that a complex consisting of this priming process, and release of MMP-9 and chemoattractants from migrated neutrophils, results in the eventual manifestation of the enhanced transmigration of eosinophils.

Neutrophils may actively participate in the development of airway disease of asthma. Our results suggest that neutrophils migrated to IL-8 may lead eosinophils to accumulate in the airways of asthma and possibly aggravate this disease. Therefore, therapies that suppress functions or accumulation of neutrophils may be effective for severe asthma. Further study will be warranted to elucidate the detailed roles of neutrophils in the pathophysiology of the disease.

**Conflict of Interest Statement:** None of the authors has a financial relationship with a commercial entity that has an interest in the subject of this manuscript.

**Acknowledgments:** The authors are thankful to Professor Masumi Akita, Ms. Noriko Mural, Assistant professor Yasushi Sakamoto, and Dr. Koji Tsuchiya for their cooperation in the studies. The authors also thank Ms. Akemi Yokote and Ms. Nozomi Nozaki for their excellent technical assistance.

## References

- Gleich GJ. Mechanisms of eosinophil-associated inflammation. *J Allergy Clin Immunol* 2000;105:651-663.
- Flood-Page PT, Menzies-Gow A, Phipps S, Ying S, Wangoo A, Ludwig MS, Barns N, Robinson D, Kay AB. Anti-interleukine-5 treatment reduces deposition of ECM proteins in the bronchial subepithelial basement membrane of mild atopic asthmatics. *J Clin Invest* 2003;112:1029-1036.
- Cowbum AS, Sladek K, Soja J, Adamek L, Nizankowska E, Szczeklik A, Lam BK, Penrose JF, Austen FK, Holgate ST, et al. Overexpression of leukotriene C4 synthase in bronchial biopsies from patients with aspirin-intolerant asthma. *J Clin Invest* 1998;101:834-846.
- Seymour ML, Rak S, Aberg D, Riise GC, Penrose JF, Kanaoka Y, Austen FK, Holgate ST, Sampson AP. Leukotriene and prostanoid pathway enzymes in bronchial biopsies of seasonal allergic asthmatics. *Am J Respir Crit Care Med* 2001;164:2051-2056.
- Wenzel SE, Szeffer SJ, Leung DYM, Sloan SI, Rex MD, Martin RJ. Bronchoscopic evaluation of severe asthma. *Am J Respir Crit Care Med* 1997;156:737-743.
- Gibson PG, Simpson JL, Salton N. Heterogeneity of airway inflammation in persistent asthma: evidence of neutrophilic inflammation and increased sputum interleukin-8. *Chest* 2001;119:1329-1336.
- Wenzel SE, Schwartz LB, Langmack EB, Halliday JL, Trudeau JB, Gibbs RL, Chu HW. Evidence that severe asthma can be divided pathologically into two inflammatory subtypes with distinct physiologic and clinical characteristics. *Am J Respir Crit Care Med* 1999;160:1001-1008.
- Pavord ID, Brightling CE, Woltmann G, Wardlaw AJ. Non-eosinophilic corticosteroid unresponsive asthma. *Lancet* 1999;353:2213-2214.
- The ENFUMOSA Study Group. The ENFUMOSA cross-sectional European multisentre study of the clinical phenotype of chronic severe asthma. *Eur Respir J* 2003;22:470-477.
- Kikuchi S, Nagata M, Kikuchi I, Hagiwara K, Kanazawa M. Association between neutrophilic and eosinophilic inflammation in patients with severe persistent asthma. *Int Arch Allergy Immunol* 2005;137: 7-11.
- Cox G. Glucocorticoid treatment inhibits apoptosis in human neutrophils: separation of survival and activation outcomes. *J Immunol* 1995;154: 4719-4725.
- Meagher LC, Cousin JM, Seckl JR, Haslett C. Opposing effects of glucocorticoids on the rate of apoptosis in neutrophils and eosinophilic granulocytes. *J Immunol* 1996;156:4422-4428.
- Teran LM, Carroll MP, Frew AJ, Redington AE, Davies DE, Lindley I, Howarth PH, Church MK, Holgate ST. Leukocyte recruitment after local endobronchial allergen challenge in asthma: relationship to procedure and to airway interleukin-8 release. *Am J Respir Crit Care Med* 1996;154:469-476.
- Teran LM, Campos MG, Begishvili BT, Schroder JM, Djukanovic R, Shute JK, Church MK, Holgate ST, Davies DE. Identification of neutrophil chemotactic factors in bronchoalveolar lavage fluid of asthmatic patients. *Clin Exp Allergy* 1997;27:396-405.
- Folkard SG, Westwick J, Millar AB. Production of interleukin-8, RANTES and MCP-1 in intrinsic and extrinsic asthmatics. *Eur Respir J* 1997;10:2097-2104.
- Lampinen M, Rak S, Venge P. The role of interleukin-5, interleukin-8 and RANTES in the chemotactic attraction of eosinophils to the allergic lung. *Clin Exp Allergy* 1999;29:314-322.
- Cassatella MA. The production of cytokines by polymorphonuclear neutrophils. *Immunol Today* 1995;16:21-26.
- Henson PM, Wenzel SE. Neutrophils and their mediators in asthma. In: Busse WW, Holgate ST, editors. *Asthma and rhinitis*. Boston: Blackwell Scientific; 2000. pp. 503-530.
- Nagata M, Sedgwick JB, Busse WW. Differential effects of granulocyte-macrophage colony-stimulating factor on eosinophil and neutrophil superoxide anion generation. *J Immunol* 1995;155:4948-4954.
- Nagata M, Yamamoto H, Shibasaki M, Sakamoto Y, Matsuo H. Hydrogen peroxide augments eosinophil adhesion via  $\beta 2$  integrin. *Immunology* 2000;101:412-418.
- Nagata M, Yamamoto H, Tabé K, Sakamoto Y. Eosinophil transmigration across VCAM-1-expressing endothelial cells is upregulated by antigen-stimulated mononuclear cells. *Int Arch Allergy Immunol* 2001; 125:7-11.
- Nordström T, Knekt M, Nordström E, Lindqvist C. A microplate-based fluorimetric assay for monitoring human cancer cell attachment to cortical bone. *Anal Biochem* 1999;267:37-45.
- Matsunaga Y, Shono M, Takahashi M, Tsuboi Y, Ogawa K, Yamada T. Regulation of lymphocyte proliferation by eosinophils via chymotrypsin-like protease activity and adhesion molecule interaction. *Br J Pharmacol* 2000;130:1539-1546.
- Schweizer RC, Welmers BA, Raaijmakers JA, Zanen P, Lammerts JW, Koenderman L. RANTES- and interleukin-8-induced responses in normal human eosinophils: effects of priming with interleukin-5. *Blood* 1994;83:3697-3704.
- Sedgwick JB, Nagata M. Mechanism of eosinophil activation. In: Busse WW, Holgate ST, editors. *Asthma and rhinitis*. Boston: Blackwell Scientific; 2000. pp. 373-393.
- Van den Steen PE, Proost P, Wuyts A, Van Damme J, Opdenakker G. Neutrophil gelatinase B potentiates interleukin-8 tenfold by aminoterminal processing, whereas it degrades CTAP-III, PF-4, and GRO-alpha and leaves RANTES and MCP-2 intact. *Blood* 2000;96:2673-2681.
- Okada S, Kita H, George TJ, Gleich GJ, Leiferman KM. Migration of eosinophils through basement membrane components *in vitro*: role of matrix metalloproteinase-9. *Am J Respir Cell Mol Biol* 1997;17:519-528.
- Levin JJ, Chen J, Du M, Hogan M, Kincaid S, Nelson FC, Venkatesan AM, Wehr T, Zask A, DiJoseph J, et al. The discovery of anthranilic acid-based MMP inhibitors. Part 2: SAR of the 5-position and P1(1) groups. *Bioorg Med Chem Lett* 2001;11:2189-2192.
- Zuurber AE, Liu L, Mul FJ, Verhoeven AJ, Knol EF, Roos D. Neutrophils enhance eosinophil migration across monolayers of lung epithelial cells. *Clin Exp Allergy* 2001;31:444-452.
- Ferrante A. Activation of neutrophils by interleukins-1 and -2 and tumor necrosis factors. *Immunol Ser* 1992;57:417-436.
- Wardlaw AJ, Hay H, Cromwell O, Collins JV, Kay AB. Leukotrienes, LTC<sub>4</sub> and LTB<sub>4</sub> in bronchoalveolar lavage in bronchial asthma and other respiratory diseases. *J Allergy Clin Immunol* 1989;84:19-26.



32. Wenzel SE, Trudeau JB, Westcott JY, Beam WR, Martin RJ. Single oral dose of prednisone decreases leukotriene B<sub>4</sub> production by alveolar macrophages from patients with nocturnal asthma but not control subjects: relationship to changes in cellular influx and FEV<sub>1</sub>. *J Allergy Clin Immunol* 1994;94:870-881.
33. Goadby P, Kelly CA, Duddridge M, Ward C, Hendrick DJ, Walters EH. Platelet-activating factor in bronchoalveolar lavage fluid from asthmatic subjects. *Eur Respir J* 1990;3:408-413.
34. Tillie-Leblond I, Pugin J, Marquette CH, Lamblin C, Saulnier F, Brichet A, Wallaert B, Tonnel AB, Gosset P. Balance between proinflammatory cytokines and their inhibitors in bronchial lavage from patients with status asthmatics. *Am J Respir Crit Care Med* 1999;159:487-494.

## Differential Effects of Salbutamol and Montelukast on Eosinophil Adhesion and Superoxide Anion Generation

Mariko Kushiya Keiko Saito Izumi Kikuchi Takehito Kobayashi  
Koichi Hagiwara Minoru Kanazawa Makoto Nagata

Department of Respiratory Medicine, Saitama Medical School, Saitama, Japan

### Key Words

$\beta_2$ -Agonist · Cell adhesion · Eosinophil · Leukotriene antagonist · Superoxide anion

### Abstract

**Background:**  $\beta_2$ -Agonists, a representative class of bronchodilators used for asthma, have been shown to modulate some functions of eosinophils, including cell adhesion. Similarly, a leukotriene receptor antagonist (LTRA) may be beneficial in controlling inflammation in asthma, as cysteinyl leukotrienes (cysLTs) can cause accumulation or activation of eosinophils. Recent evidence suggests that the addition of an LTRA, but not a long-acting  $\beta_2$ -agonist, to inhaled corticosteroid additionally reduces the number of eosinophils in sputum and blood from patients with asthma. The present study examined whether a  $\beta_2$ -agonist and an LTRA differentially modify eosinophil adhesion and activation induced by cysLTs and other activators. **Methods:** Eosinophils were isolated from blood of healthy donors and then incubated in the presence or absence of salbutamol (albuterol) or montelukast. Eosinophils were then exposed to leukotriene D<sub>4</sub> (LTD<sub>4</sub>) or another activator, and the generation of superoxide anion (O<sub>2</sub><sup>-</sup>) was evaluated by cytochrome C reduction assay. Eosinophil adhesion was examined

by an eosinophil peroxidase assay. **Results:** Montelukast, but not salbutamol (both at 1  $\mu$ M), inhibited LTD<sub>4</sub>-induced (100 nM) eosinophil adhesion to recombinant human intercellular adhesion molecule 1. Both drugs similarly and partially inhibited the 100 pM interleukin-5-induced adhesive response of eosinophils to recombinant human intercellular adhesion molecule 1. Montelukast, but not salbutamol, blocked LTD<sub>4</sub>-induced eosinophil O<sub>2</sub><sup>-</sup> generation of eosinophils. Finally, neither salbutamol nor montelukast modified phorbol myristate acetate (1 ng/ml)-induced O<sub>2</sub><sup>-</sup> generation from eosinophils. **Conclusion:** These results confirm that LTD<sub>4</sub> directly induces activation of eosinophils via the cysLT1 receptor. Furthermore, the results suggest that a  $\beta_2$ -agonist has no effect on eosinophil adhesion and activation induced by cysLTs. These results explain the differential effects of an LTRA and a  $\beta_2$ -agonist in the treatment of eosinophilic inflammation in asthma.

Copyright © 2006 S. Karger AG, Basel

### Introduction

Eosinophils preferentially accumulate at sites of allergic inflammation and are believed to play a role in the pathophysiology of asthma. Recent studies have estab-

KARGER

Fax +41 61 306 12 34  
E-Mail karger@karger.ch  
www.karger.com

© 2006 S. Karger AG, Basel  
1018-2438/06/1405-0017\$23.50/0

Accessible online at:  
www.karger.com/iaa

Correspondence to: Makoto Nagata, MD  
Department of Respiratory Medicine  
38 Morohongou, Moroyama-cho, Truma-gun  
Saitama 350-0495 (Japan)  
Tel. +81 492 76 1319, Fax +81 492 95 8399, E-Mail favre4mn@saitama-mcd.ac.jp

lished that eosinophils are essentially involved in airway remodeling [1–3]. Moreover, it is theoretically conceivable that eosinophils are the major cellular source of cysteinyl leukotrienes (cysLTs) in asthma [4, 5].

Over the past decade, increasing evidence has suggested that cysLTs contribute to the accumulation of eosinophils in the airway tissues of asthmatics [6–9]. For example, leukotriene E<sub>4</sub> (LTE<sub>4</sub>) inhalation increases the accumulation of eosinophils and, to a lesser extent, neutrophils in asthmatic individuals [6]. In this context, cysLTs exert various effects on human eosinophils *in vitro* [10–16]. We have reported that LTD<sub>4</sub> upregulates the expression of  $\beta_2$ -integrins on human eosinophils *in vitro* and augments eosinophil adhesion to tissue culture plates or to recombinant human intercellular cell adhesion molecule 1 (rh-ICAM-1) [11]. Furthermore, we observed that LTD<sub>4</sub> directly induces transendothelial migration, respiratory burst and degranulation, mainly via the cysLT1 receptor and  $\beta_2$ -integrin [12]. Clinical studies have examined whether leukotriene receptor antagonists (LTRAs) modulate eosinophil accumulation in the asthmatic airway. For example, pranlukast, a cysLT1 antagonist, reduces the number of eosinophils in the bronchial mucosa [17] and in sputum [18]. Montelukast, another LTRA, yielded similar results [19].

$\beta_2$ -Agonists, a representative class of antiasthma drugs, can downmodulate some functions of eosinophils [20]. For example, we have reported that tulobuterol, a  $\beta_2$ -agonist, attenuates interleukin (IL)-5-induced adhesion of blood eosinophils [21]. Therefore, like an LTRA, a  $\beta_2$ -agonist may act to regulate eosinophilic inflammation in asthma. However, recent evidence suggests that the combination of inhaled corticosteroid (ICS) plus an LTRA exerts marked antieosinophilic or anti-inflammatory effects in asthma, as compared with an ICS/long-acting  $\beta_2$ -agonist (LABA) combination [22, 23], suggesting that eosinophilic inflammation induced by cysLTs in asthma may be insensitive to  $\beta_2$ -agonists. The present study was undertaken to examine whether  $\beta_2$ -agonists and LTRAs differentially modify eosinophil adhesion or activation induced by cysLTs and other activators.

## Materials and Methods

### Reagents

Percoll was obtained from Pharmacia (Uppsala, Sweden). Anti-CD16 antibody-coated magnetic beads were purchased from Miltenyl Biotec (Auburn, Calif., USA). RPMI-1640 medium, PBS, newborn calf serum and fetal calf serum (FCS) were obtained from Life Technologies (Grand Island, N.Y., USA). LTD<sub>4</sub> was obtained from

Cayman Chemical (Ann Arbor, Mich., USA), montelukast was provided by Merck & Co., Inc. (White Station, N.J., USA), and rh-IL-5 and rh-ICAM-1 were purchased from R&D Systems (Minneapolis, Minn., USA). Other reagents were purchased from Sigma (St. Louis, Mo., USA) unless stated otherwise.

### Eosinophil Separation

Eosinophils were isolated from the peripheral blood of healthy volunteers aged 20–29 years, with an equal sex distribution. Eosinophils were isolated by negative immunomagnetic bead selection as described previously [24, 25]. Briefly, heparinized blood diluted with Hank's balanced salt solution (HBSS) without Ca<sup>2+</sup> was separated by centrifugation for 20 min at 700 g over 1.090 g/ml Percoll. Plasma, mononuclear cells and the Percoll were removed, and pelleted red blood cells were lysed by hypotonic shock. The resulting granulocytes were washed in HBSS supplemented with 2% newborn calf serum at 4°C and then incubated with anti-CD16 antibody-coated magnetic beads for 40 min at the same temperature. The cells were filtered through steel wool in a magnetic field (Miltenyl Biotec) to remove neutrophils bound to the magnetic beads. CD16-negative eosinophils (>98% purity and >99% viability) were collected, washed and resuspended in RPMI supplemented with 5% FCS (RPMI/FCS).

### Eosinophil Adhesion Assay

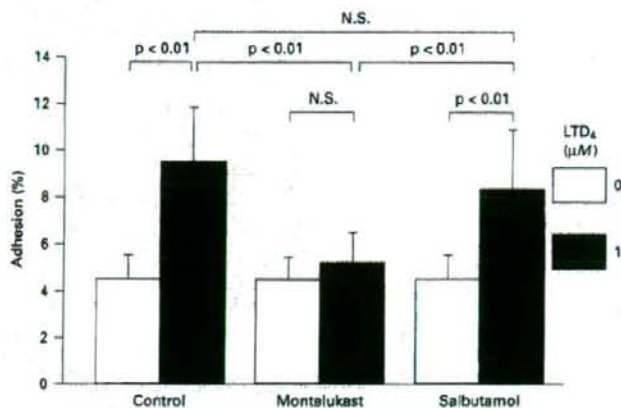
Eosinophil adhesion to rh-ICAM-coated plates was assessed as residual eosinophil peroxidase (EPO) activity of adherent eosinophils, as previously described [11, 21, 26]. Briefly, rh-ICAM-1 was dissolved in 0.05 M NaHCO<sub>3</sub> coating buffer (15 mM NaHCO<sub>3</sub>, 35 mM Na<sub>2</sub>CO<sub>3</sub>, pH 9.2), added to 96-well tissue culture plates (Corning Incorporated, Corning, N.Y., USA) and incubated at 4°C overnight [11]. Residual fluid was decanted and 200  $\mu$ l/well HBSS/0.1% gelatin (HBSS/gel) was added to reduce nonspecific adhesion. After a 2-hour incubation at ambient temperature, the wells were decanted and ready for the addition of eosinophils [11]. Eosinophils (100  $\mu$ l of  $1 \times 10^5$  cells/ml in HBSS/FCS) were preincubated with either montelukast (1  $\mu$ M), salbutamol hemisulfate (1  $\mu$ M) or buffer alone (control) at 37°C for 20 min and then placed onto rh-ICAM-1-coated plates in the presence or absence of an activator and incubated for 20 min at 37°C.

After five washes with 37°C HBSS, 100  $\mu$ l HBSS/FCS was added to the reaction wells. In the experiments to determine kinetics, the reaction was serially stopped by partial aspiration and washing of the corresponding wells every 5 min for the first 10 min and every 10 min for the next 50 min. As standards, 100  $\mu$ l of serially diluted cell suspensions ( $1 \times 10^3$ ,  $3 \times 10^3$ ,  $1 \times 10^4$ ,  $3 \times 10^4$  and  $1 \times 10^5$  cells/ml) were added to empty wells. EPO substrate (1 mM *o*-phenylenediamine, 1 mM H<sub>2</sub>O<sub>2</sub> and 0.1% Triton X-100 in Tris buffer, pH 8.0) was then added to all wells. After 30 min incubation at room temperature, 50  $\mu$ l of 4 M H<sub>2</sub>SO<sub>4</sub> was added to stop the reaction, and the absorbance at 490 nm was measured. Each experiment was performed in quadruplicate using eosinophils from a single donor, and the mean value was used to determine the percentage of eosinophil adhesion, which was calculated from the log dose-response curve. Eosinophil viability after incubation exceeded 98% by trypan blue dye exclusion.

### Superoxide Anion Generation

Eosinophil superoxide anion (O<sub>2</sub><sup>-</sup>) generation was measured as the superoxide dismutase (SOD)-inhibitable reduction in ferricy-

**Fig. 1.** Effects of montelukast (1  $\mu$ M) and salbutamol (1  $\mu$ M) on LTD<sub>4</sub>-induced (100 nM) eosinophil adhesion to rh-ICAM-1. Data are expressed as means  $\pm$  SEM from six experiments. N.S. = Not significant.



tochrome C in 96-well culture plates (Corning Inc.), as described previously [12, 26]. We initially added SOD (0.2 mg/ml in HBSS/gel; 20  $\mu$ l) to SOD control wells and then HBSS/gel to all wells to bring the final volume to 100  $\mu$ l. Eosinophil density was adjusted to  $1.25 \times 10^6$  cells/ml of HBSS/gel mixed 4:1 with cytochrome C (12 mg/ml HBSS/gel), and then eosinophils, which were preincubated with either montelukast (1  $\mu$ M), salbutamol hemisulfate (1  $\mu$ M) or buffer alone (control) at 37°C for 20 min, were added to all wells in a volume of 100  $\mu$ l. To initiate the reaction, the cells were incubated with LTD<sub>4</sub> (100 nM) or phorbol myristate acetate (PMA; 1 ng/ml). Immediately after adding the activator, the absorbance of the cell suspensions in the wells was measured at 550 nm in an Immuno-Mini (NJ-2300; Japan Intermed Co., Tokyo, Japan), followed by repeated readings over the next 240 min. Between readings, the plates were placed in a 5% CO<sub>2</sub> incubator at 37°C. Each reaction was performed in duplicate against an identical control reaction containing 20  $\mu$ g/ml SOD. The results were adjusted to represent a 1-ml reaction volume, and O<sub>2</sub> generation was calculated at an extinction coefficient of  $21.1 \times 10^3$  M<sup>-1</sup> cm<sup>-1</sup> as nanomoles of cytochrome C reduced per  $1.0 \times 10^6$  cells per minute minus the SOD control. The maximum value during the incubation time was examined for the effects of drugs on eosinophil O<sub>2</sub> generation. Cell viability determined by trypan blue exclusion at the completion of each experiment remained at 95% after 240 min of incubation.

#### Statistics

Data are presented as means  $\pm$  SEM. ANOVA with repeated measures was used to compare more than two variables. When the initial p value was below 0.05, Scheffe's post-hoc test was used to determine the significance of differences between groups. Student's t test was used to perform paired comparisons. Statistical significance was established at the p < 0.05 level.

#### Results

As previously reported, 100 nM LTD<sub>4</sub> augmented the adhesive response of eosinophils to rh-ICAM-1 (fig. 1). Montelukast, at a clinically relevant concentration (1  $\mu$ M), significantly inhibited LTD<sub>4</sub>-induced eosinophil adhesion to rh-ICAM-1 (p < 0.01, n = 6; fig. 1). In contrast, salbutamol (1  $\mu$ M) did not modify this adhesion of eosinophils (p > 0.1, n = 6; fig. 1). Neither montelukast nor salbutamol modified the spontaneous adhesion of eosinophils to rh-ICAM-1 (p > 0.1, respectively, n = 6; fig. 1).

In contrast to the differential effects observed with LTD<sub>4</sub>-induced adhesion, both montelukast and salbutamol (1  $\mu$ M) similarly and partially inhibited the 100 pM IL-5-induced adhesive response of eosinophils to rh-ICAM-1 (p < 0.01, respectively, n = 6; fig. 2). There was no statistically significant difference between the effects of montelukast and salbutamol (p > 0.1).

As previously reported, 100 nM LTD<sub>4</sub> directly induced the generation of O<sub>2</sub> from eosinophils. This activation was significantly inhibited by montelukast (1  $\mu$ M) (p < 0.01, n = 6; fig. 3a). On the other hand, montelukast did not modify PMA-induced (1 ng/ml) generation of O<sub>2</sub> from eosinophils (p > 0.1, n = 6; fig. 3b). Salbutamol (1  $\mu$ M) did not modify LTD<sub>4</sub>- or PMA-induced O<sub>2</sub> generation from eosinophils (p > 0.1, respectively, n = 6; fig. 4a, b). The baseline spontaneous generation of O<sub>2</sub> from eosinophils was not modified by montelukast or salbutamol (data not shown).